CONSTRUCTION MATERIALS CONSULTANTS, INC.

# Laboratory Analyses Of A Masonry Mortar From A Late 19th Century Historic Church in Pittsburgh, Pennsylvania

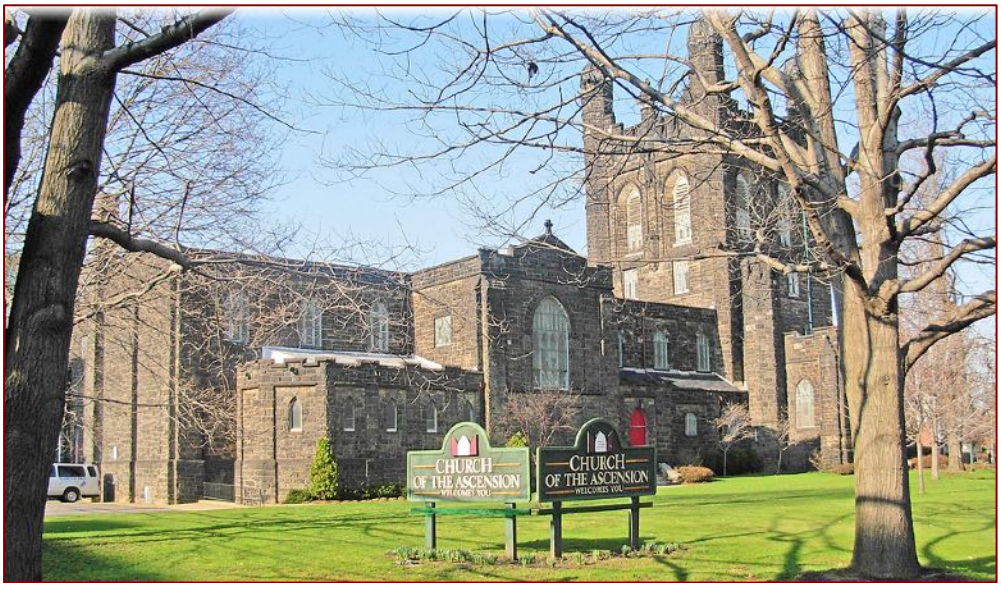


Church of the Ascension
4729 Ellsworth Avenue
Pittsburgh, PA 15213

May 25, 2020
CMC 0520120

## TABLE OF CONTENTS

# LABORATORY STUDIES OF A HISTORIC MASONRY MORTAR FROM CHURCH OF THE ASCENSION, PITTSBURGH, PENNSYLVANIA

## ABSTRACT

The present study involves evaluation of a historic masonry mortar sample from Church of the Ascension located at Ellsworth Avenue and Neville Street in the Shadyside neighborhood of Pittsburgh, Pennsylvania. Built in 1898, the church was added to the List of Pittsburgh History and Landmarks Foundation Historic Landmarks in 1971.

As part of the renovation process, multiple pieces of an original masonry mortar from the church was provided for detailed laboratory investigations to determine the type, composition, and microstructure of the mortar, including the type, grain-size distribution, and mineralogical composition of sand used in the mortar, type(s), chemical, and mineralogical compositions of the binder(s) added, microstructural evidence of any physical and/or chemical deterioration of the mortar from exposures, volumetric proportions of binder(s) and sand ingredients in the mix, and finally, suggestions for a suitable mix to match with the original mortar used during the late 19$^{th}$ century.

Mortar was analyzed by comprehensive laboratory examinations following various industry standards, e.g., ASTM C 1324 and RILEM methods starting with visual examinations, extensive optical microscopy, scanning electron microscopy and energy-dispersive X-ray microanalyses (SEM-EDS), grain-size distribution of sand extracted from the mortar by acid-digestion, followed by wet chemical analyses, X-ray diffraction (XRD), X-ray fluorescence (XRF), thermal analyses (TGA, DTG, DSC), and finally ion chromatography of water-soluble anions extracted from the mortar.

Based on these studies, **the mortar is determined to be made using natural cement *aka* Rosendale cement, dolomitic lime (most probably used as lime putty), and a mixed sand consisting of crushed siliceous (quartz, quartzite) sand and natural (rounded) sand of dominantly argillaceous (shale, siltstone) and ferruginous components**.

Natural cement was manufactured from calcination of an impure (argillaceous) dolomitic limestone without any subsequent slaking, whereas dolomitic lime was manufactured by calcination of a relatively pure dolomitic limestone followed by slaking in excess water.

**The estimated volumetric proportion of natural cement to lime to sand is determined to be 1-part natural cement to less than 2-part lime to 7-part sand**. Sand content is about 2 1/2 times the sum of separate volumes of cement and lime, which is consistent with the commonly recommended 2 1/4 to 3 times sand in modern masonry mortars.

Sand extracted from the mortar after acid digestion showed an overall dark color tone of many sand particles from use of appreciable amounts of argillaceous and ferruginous components in the sand. Grain size distribution of sand showed relatively finer size of sand than size distribution of modern masonry sand as specified in ASTM C 144. Dominance of argillacoeus (shale, argillaceous silstone) components in sand are potentially deleterious to volume instability of mortar during exposures to moisture. Too much clay-rich components in sand increases the water demand of mortar mix and risk of unsoundness during exposures to mosture, wetting and drying, and freezing and thawing cycles during exposures in a moist outdoor environment. Angular quartz and rounded shale particles in sand indicates incorportaiton of crushed silica sand and natural river sand, respectively.

Optical and SEM-EDS analyses of paste has confirmed the presence of natural cement made using calcination of impure dolomitic limestone where many residual natural cement particles retained the original rhombic crystal shapes of dolomite grains in original dolomitic limestone feed (with evidence of elemental migraiton during calcination process e.g., from reddish-brown iron enrichment at the rims of dolomite grains to high-temperature silica polymorphs as fine insterstitial grains between calcined dolomite grains), and, dolomitic lime as the binder components.

The examined historic mortar, however, cannot be compared with a modern equivalent Portland cement-lime mortar due to use of natural cement, and extensive chemical alteration (lime leaching) of the historic mortar found in optical microscopy and SEM-EDS studies, which has severely affected the mix calculations. In fact, mix

calculations recommended in ASTM C 1324 are applicable only for the modern ASTM C 270 cement-lime and masonry cement mortars, which cannot be extended for historic lime mortars or natural cement-lime mortars let alone after extensive alterations, e.g., lime leaching that are common in historic mortars. The type of ingredients and use of natural cement and lime putty in the calculated proportions are consistent with many historic natural cement-lime mortars used in many historic masonry construction projects in Pittsburgh during mid-to-late-19$^{th}$ century.

Fine-grained severely carbonated lime-rich paste, lime leaching of paste leaving silica-alumina-iron-rich residue, sporadic isolated occurrences of residual natural cement particles showing relic dolomite rhombs in semi-amorphous calcium-aluminate-silicate matrix of natural cement, occasional lime lumps, and many other microstructural features that are common in many 19$^{th}$ century mortars are found in the present sample that are telltale features of natural chemical alterations of a historic masonry mortar made using natural cement and lime as the two essential binders.

Based on the determined compositions of binders and sand, and estimated mix proportion, **a suitable tuck-pointing mortar could be formulated by incorporating a modern natural cement (similar to Rosendale 10C cement from Edison Coatings, Inc.), hydrated lime, and a dominantly siliceous (quartz-rich) sand – all in conformance to the specifications of ASTM C 10, C 207, and C 144, respectively**.

Avoid using a sand containing appreciable proportions of argillaceous and ferruginous components since these are potentially deleterious to long-term durability and serviceability of mortar in a moist outdoor environment. Sand should be sound, preferably siliceous in nature. For a color match to the dark gray color tone of sand in the existing mortar (where dark tone was from use of dark gray shale and ferruginous particles in sand) a dark crushed calcareous (limestone) component can be added in the sand. The mixed sand must confirm to ASTM C 144 specification for masonry sand.

The exact proportions of cement to lime to sand should be determined by trials and errors starting with a mix similar to a modern equivalent of ASTM C 270 Type N or S cement-lime mortar (depending on the masonry units) but using natural cement instead of Portland cement), and testing on a small test area to match in appearance, compositions, and properties with the existing mortar.

## INTRODUCTION

Church of the Ascension (Figure 1) is located at Ellsworth Avenue and Neville Street in the Shadyside neighborhood of Pittsburgh, Pennsylvania. Built in 1898, the church was added to the List of Pittsburgh History and Landmarks Foundation Historic Landmarks in 1971.

As part of the renovation process, multiple pieces of the original masonry mortar from the church were provided for detailed laboratory investigations to determine the type, composition, and microstructure of the mortar, including the type, grain-size distribution, and mineralogical composition of sand used in the mortar, type(s), chemical, and mineralogical compositions of the binder(s) added, microstructural evidence of any physical and/or chemical deterioration of the mortar from exposures, volumetric proportions of binder(s) and sand ingredients in the mix, and finally, suggestions for a suitable mix to match with the existing mortar.

Total weight of mortar received is 333.5 grams. The largest piece measures 80 mm × 50 mm × 16 mm in length × width × thickness (Fig. 2, 3). All pieces are similar in appearance (with no evidence of any accidental inclusion of a different mortar type), medium brownish toned, and moderately hard. Representative portions from coarser fractions were selected for various instrumental techniques, e.g., optical and electron microscopy and microanalyses, X-ray diffraction and X-ray fluorescence, chemical analyses (soluble silica content, insoluble residue, loss on ignition, and ion chromatography), sand extraction and sieve analysis, and thermal analyses. Finest fraction passing US No. 50 sieve (<0.3 mm in size) was selected for X-ay diffraction and X-ray fluorescence studies for bulk mineralogy and chemical composition, respectively.

Figure 1: Church of the Ascension, Pittsburgh, PA

Figure 2: Mortar sample, as received.

## METHODOLOGIES[1]

Until 1970-1980, characterization of masonry mortars were mostly based on traditional wet chemical analysis (Jedrzejewska, 1960, Stewart and Moore, 1981) where interpretation of results were often difficult if not impossible without a good knowledge of the nature of different ingredients. The majority of later characterization proposed optical microscopy (Erlin and Hime 1987, Middendorf et al. 2000, Elsen 2006) as the first step in identification of different components or mortar based on which other analytical techniques including wet chemistry are performed, e.g., scanning electron microscopy and X-ray microanalysis, X-ray diffraction, X-ray fluorescence, atomic absorption, thermal analysis, infrared spectroscopy, etc. (Bartos et al. 2000, Elsen 2006, Callebaut et al. 2000, Erlin and Hime 1987, Goins 2001, 2004, Groot et al. 2004, Doebley and Spitzer 1996, Chiari et al. 1996, Middendorf et al. 2000, 2004, 2005, Leslie and Hughes 2001, Martinet and Quenee 2000, Valek et al., 2012, Jana 2005, 2006).

[1] For details on laboratory facilities for testing of masonry mortar, visit www.cmc-concrete.com.

The choice of appropriate analytical technique depends mainly on the questions that have to be addressed, and, on the amount of material available.

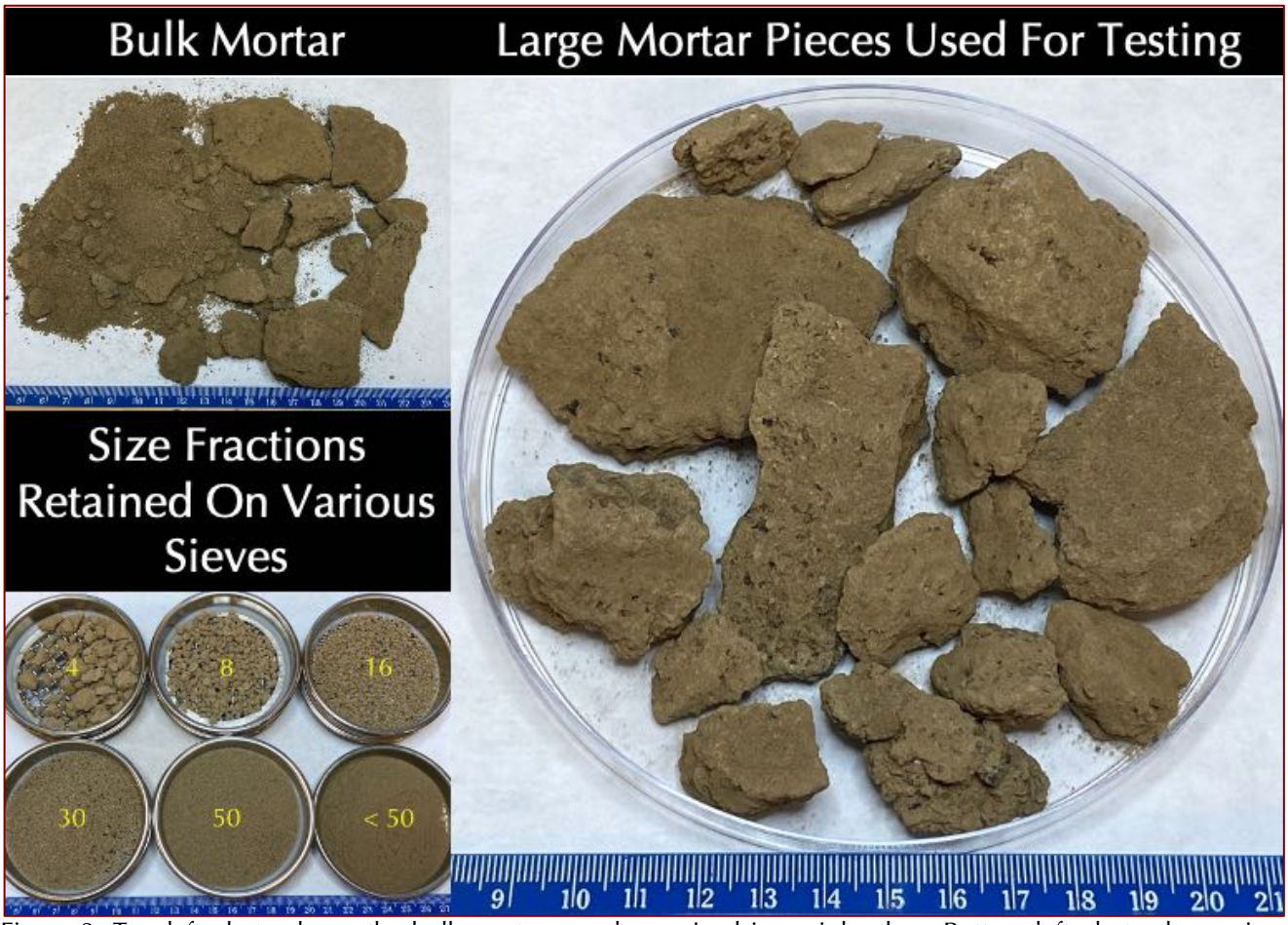


Figure 3: Top left photo shows the bulk mortar sample received in a ziploc bag. Bottom left photo shows size fractions of mortar retained on various US sieves of which fraction finer than US No. 50 sieve (i.e. <0.297 mm) was used for X-ray diffraction and X-ray fluoresence studies for mineralogy and chemical composition of fine fraction of mortar. Right photo shows coarse fragments used for optical and electron microscopy, wet chemical analysis, and sand extraction for sieve analyses of sand.

Purposes of laboratory testing are: (a) to document a historic or modern masonry mortar by examining its sand and binder components, proportions of various ingredients, and their effects on properties and performance of the mortar, (b) evidence of any chemical or physical deterioration of mortar from unsoundness of its ingredients to effects of potentially deleterious agents from the environment (e.g., salts), (c) records of later repointing events and their beneficial or detrimental effects on the performance of the original mortar and masonry units, and finally, (d) an assessment of an appropriate restoration mortar to ensure compatibility with the existing mortar.

Currently there are two standardized procedures available that describe various laboratory techniques for analyses of masonry mortars with special emphases on historic mortars. One is ASTM C 1324 "Standard Test Method for Examination and Analysis of Hardened Masonry Mortar," which includes detailed petrographic examinations, followed by chemical analyses, along with various other analytical methods to test masonry mortars as described in various literatures, e.g., XRD, thermal analysis, and infrared spectroscopy. The second one is the RILEM method described in Middendorf et al. (2004, 2005).

The present mortar was tested by following these established methods of ASTM C 1324, and RILEM, which include detailed petrographic examinations i.e. optical and scanning electron microscopy and X-ray microanalyses (SEM-EDS), followed by chemical analyses (gravimetry, acid digestion), X-ray fluorescence (XRF), X-ray diffraction (XRD),

and thermal analyses (TGA, DTG, and DSC). Mortar sample was first photographed with a digital camera, scanned on a flatbed scanner, and examined in a low-power stereomicroscope for the preliminary examinations, e.g., to screen any unusual pieces having different appearances, e.g., representing contaminants from prior pointing episodes. Representative subset pieces of interest are then selected for: (a) optical microscopy and (b) scanning electron microscopy and X-ray microanalysis for chemical and mineralogical compositions, and microstructures of sand, paste, and overall mortar, (c) acid digestion, preferably from un-pulverized or lightly pulverized sample for sand extraction for grain size distribution, (d) loss on ignition from ambient to 950°C temperatures for free and hydrate water, and carbonate contents, (e) acid digestion for determination of insoluble residue content, (f) cold acid and hot alkali digestions for determination of soluble silica content from hydraulic binder if any, after pulverizing a subset to finer than 0.3 mm size, and, (g) ultra-fine pulverization (<44-micron) of a subset for XRD, XRF, and thermal analysis. Any additional analyses, if needed, e.g., water digestion of mortar for determination of water-soluble salts by ion chromatography, or, Fourier-transform infrared spectroscopy of mortar for determining any organics added, etc. are done on as-needed basis from the remaining set.

Information obtained from petrographic examinations is crucial to devise appropriate guidelines for chemical methods, and, to properly interpret the results of chemical analyses. For example, detection of siliceous versus calcareous versus argillaceous components of aggregates in sample, or, the presence of any pozzolan in the binder (slag, fly ash, ceramic dusts, etc.) from petrography restricts which chemical method to follow, and how to interpret the results of such analyses, e.g., acid-insoluble residue contents. Therefore, a direct chemical analysis e.g., acid digestion of a mortar without doing a prior petrographic examination to determine the types of aggregates and binder used could lead to highly erroneous results and interpretation. Armed with petrographic and chemical data, and based on assumed compositions and bulk densities of the sand and the binder(s) similar to the ones detected from petrographic examinations, volumetric proportions of sand and various binders present in the examined sample can be calculated. The estimated mix proportions from such calculations can provide a rough guideline to use as a starting mix for mock-up mix during formulation of a pointing mortar to match with the existing mortar.

## Optical Microscopy

The main purposes of optical microscopy of masonry mortar are characterization of: (a) aggregates, e.g., type(s), chemical and mineralogical compositions, nominal maximum size, shape, angularity, grain-size distribution, soundness, alkali-aggregate reactivity, etc. (b) paste, e.g., compositions and microstructures to diagnose various type(s) of binder(s) used, (c) air, e.g., presence or absence of air entrainment, air content, etc., (d) alterations, e.g., lime leaching, carbonation, staining, etc. due to interactions with the environmental agents during service, and effects of such alterations on properties and performance of mortar; and (e) deteriorations, e.g., chemical and/or physical deteriorations during service, cracking from various mechanisms, salt attacks, possible reasons for the lack of bond if reported from the masonry unit, etc. Fragments selected from preliminary examinations for microscopy are sectioned, polished, and thin-sectioned (down to 25-30 micron thickness) preferably after encapsulating and impregnating with a dyed-epoxy (Fig. 3) to improve the overall integrity of the sample during precision sectioning and grinding, and to highlight porous areas, voids, and cracks. Prepared sections are then examined in a high-power (up to 100X) Stereozoom microscope having reflected and transmitted-light, and plane and crossed polarized-light facilities, and eventually in a high-power (up to 600X) petrographic microscope equipped with transmitted, reflected, polarized, and fluorescent-light facilities. Capturing high-resolution photomicrographs from these microscopes via digital microscope cameras with image analyses software are an integral part of documentations during petrographic examinations.

Therefore, four essential steps followed during optical microscopy are: (a) visual examination of as-received, fresh fractured, and sectioned surfaces of mortar in a stereo-microscope, (b) preparation of a large-area (50 × 75 mm) thin section of homogeneous thickness (25-30 micron), (c) observation of thin section in a transmitted-light stereo-zoom microscope from 5X to 100X preferably with polarized-light facilities to observe large-scale distribution of sand and mortar microstructure, and finally (d) observation of thin section in a polarized-light (petrographic) microscope from 40X to 600X equipped with transmitted and reflected polarized and fluorescent-light facilities for examinations of sand and binder compositions and microstructures.

For thin section preparation, representative fragments are oven-dried at 40°C to a constant mass and placed in a flexible (e.g., molded silicone) sample holder, then encapsulated with a colored dye-mixed (e.g., blue dye commonly used in sedimentary petrography, or, fluorescent dye, Elsen 2006) low-viscosity epoxy resin under vacuum to impregnate the capillary pore spaces of mortar, improve the overall integrity of sample during sectioning by the cured epoxy, highlight porous areas of mortar, alterations, cracks, voids, reaction products, etc. The epoxy-encapsulated cured solid block of sample is then de-molded, sectioned if needed, and processed through a series of coarse to fine grinding on metal and resin-bonded diamond grinding discs with water or a lubricant, eventually a perfectly flat clean ground surface is glued to a frosted large-area (50 × 75 mm) glass slide. Careful precision sectioning and precision grinding of the sample is then done in a thin-sectioning machine till the thickness is down to 50 to 60 micron. Final thinning down to 25 to 30 micron thickness is done on a glass plate with fine (15 micron) alumina abrasive. Thin section is eventually polished with various fine (1 micron to 0.25 micron size) diamond abrasives on polishing wheels suitable for examinations in a petrographic microscope, and eventually in SEM-EDS. Sample preparation steps are described in Jana (2006).

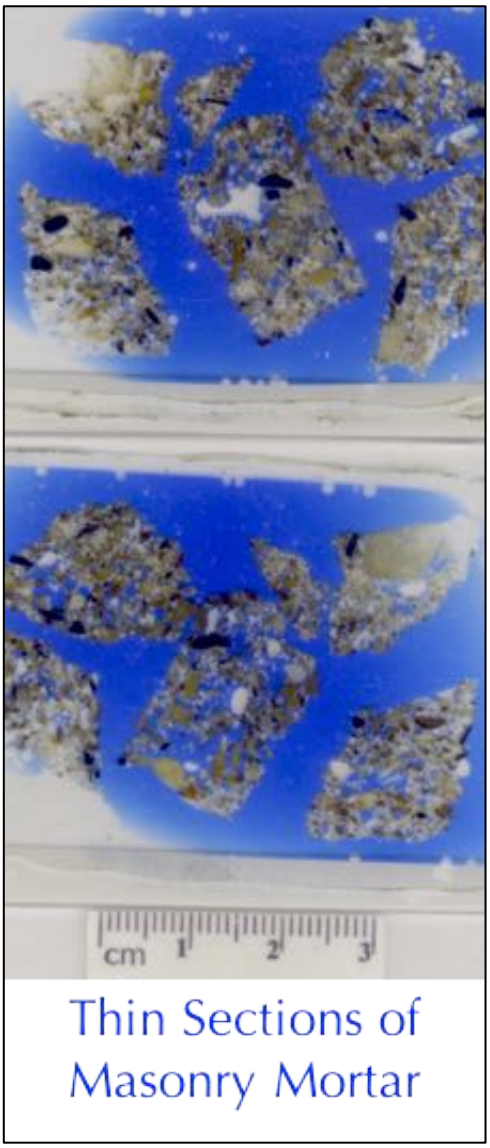


Figure 4: Blue dye-mixed epoxy-impregnated large-area (50 × 75 mm size) thin section prepared for microscopy.

More elaborate steps followed during optical microscopy include: (a) visual examinations of sample as-received to select fragments for detailed optical microscopy; initial digital and flatbed scanner photography of sample as-received; (b) low-power stereomicroscopic examinations of saw-cut and freshly fractured sections of sample for evaluation of variations in color, grain-size and appearances of sand, and the nature of the paste; (c) examinations of oil immersion mounts for special features and materials in a petrographic microscope; (d) examinations of colored (blue or fluorescent) dye-mixed epoxy-impregnated polished thin sections in a transmitted-light Stereozoom microscope for determination of size, shape, angularity, and distribution of sand, as well as abundance and distribution of void and pore spaces that are highlighted by the colored dye-mixed epoxy; (e) image analyses of photomicrographs of thin sections for estimations of pores, voids, intergranular open spaces, and shrinkage microcracks by using Image J or other image analysis software where multiple photomicrographs are collected in plane polarized light mode by using a high-resolution Stereozoom microscope equipped with transmitted and polarizing light facilities and stitched to get an adequate representative coverage; (f) examinations of colored (blue or fluorescent) dye-mixed epoxy-impregnated polished thin sections in a petrographic microscope for detailed compositional, mineralogical, textural, and microstructural analyses of aggregates and binders, along with diagnoses of evidence of any deleterious processes and alterations (e.g., lime leaching, precipitation of secondary deposits and alteration products, salts); (g) examinations of polished thin or solid section in reflected-light (epi-illumination) mode of petrographic microscope after etching the surface with acids to identify various non-hydrated hydraulic phases (e.g., $C_2S$, $C_3S$, $C_3A$, etc., Middendorf et al., 2005); (h) examinations of any physical or chemical deterioration or signs of improper construction practices from microstructural evidences; (i) stereo-microscopical examinations of size, shape, and color variations of sand extracted after hydrochloric acid digestion; and finally (j) selection of areas of interest to be examined by scanning electron microscopy.

## Scanning Electron Microscopy & Microanalysis by Energy-Dispersive X-ray Spectroscopy (SEM-EDS)

Methods followed in SEM-EDS include: (a) secondary electron imaging (SEI) to determine the microstructure and morphology of the examined surface of sample, (b) backscatter electron (BSE) imaging to determine compositions of various phases from various shades of darkness/grayness/brightness from average atomic numbers of phases from the darkest pore spaces to brightest iron minerals (e.g., thaumasite, periclase, ettringite, quartz, dolomite, monosulfate, gypsum, calcite, C-S-H, aluminate, calcium hydroxide, belite, alite, free lime, and ferrite having progressively increasing average atomic numbers and brightness in BSE image), (c) X-ray elemental mapping (dot mapping) of an area of interest to differentiate various phases, (d) point-mode or area (raster)-mode analysis of specific area/phase of interest on a polished thin or solid section, and (e) average compositional analysis of a specific phase or an area on a polished thin or solid section or small subset of a sample.

The main purposes of SEM-EDS studies are to: (a) observe the morphologies and microstructures of various phases of sand and binder, (b) characterize the typical fine-grained microstructure of hydrated, carbonated, and hydraulic components of binder that are too fine to be examined by optical microscopy and are not well crystallized to be detected by XRD; (c) determine major element oxide compositions, and compositional variations of paste, and from that determine the type of binder(s) used, especially to differentiate non-hydraulic calcitic and dolomitic lime mortars from hydraulic lime varieties (e.g., from silica contents of paste), natural cements (e.g., from silica and magnesia contents), pozzolans, slag cements, Portland cements, etc. all from their characteristic differences in compositions and hydraulicities (e.g., cementation index of Eckel 1922); (d) determine composition of residual hydraulic phases to assess the raw feed and calcination processes used in manufacturing of binder; (e) assess hydration, carbonation, and alteration products of binders, (f) investigate effects of various alterations of paste during service and its role on properties and performance of mortar, (g) detect salts and other potentially deleterious constituents, (h) detect pigments and fillers, (i) examine compositional variations across multiple mortars installed, etc.; and eventually (j) complement and confirm the results of optical microscopy.

Due to characteristic difference in compositions of pastes made using various binders, e.g., non-hydraulic lime (CaO dominates over all other oxides), variably hydraulic lime (CaO with variable $SiO_2$ contents depending on degree of hydraulicity), dolomitic lime (high CaO and MgO), natural cement (CaO, $SiO_2$, $Al_2O_3$, and MgO contents are high, high MgO and FeO contents are characteristic), and Portland cement (CaO and $SiO_2$ contents are higher than all other oxides), SEM-EDS analysis of paste is a powerful method for detection of the original binder components in the sample. Effects of chemical alterations and various chemical deteriorations of a mortar (e.g., lime leaching, secondary calcite precipitates, gypsum deposits, etc.) can also be detected by SEM-EDS.

SEM-EDS analysis was done in a CamScan Series 2 scanning electron microscope equipped with a high-resolution column 40Å tungsten, 40 kV electron optics zoom condenser 75° focusing lens operating at 20 kV, equipped with a variable geometry secondary electron detector, backscatter electron detector, EDS detector for observations of microstructures at high-resolution, compositional analysis, and quantitative determinations of major element oxides from various areas of interest, respectively. Revolution 4Pi software was used for digital storage of secondary electron and backscatter electron images, elemental mapping, and compositional analysis along a line, or on a point or an area of interest. Portion(s) of interest on the polished 50 mm × 75 mm size thin section used for optical microscopy were subsequently coated with carbon or gold-palladium film and placed on a custom-made aluminum sample holder to fit inside the large multiported chamber of CamScan SEM equipped with the eucentric 50 × 100 mm motorized stage. Usually, features of interest from optical microscopy are marked on the thin section with a fine-tipped conductive marker pen for further observations in SEM. Alternately, solid polished section or grain mount from phases or areas of interest can also be examined. Procedures for SEM examinations are described in ASTM C 1723 and Sarkar et al. (2000).

## Acid Digestion

Acid digestion is perhaps the most commonly used test of masonry mortar, which is done to: (a) extract sand from sample by dissolving out the binder fractions so that grain-size distribution of sand can be done by sieve analysis, and (b) assess insoluble sand content in the sample. Sand content after acid digestion is determined both from: (a) 1.00 gram of pulverized sample (finer than 0.3 mm size) digested in 50-ml dilute (1+3) HCl (heated rapidly but below boiling), and, (b) from digesting a representative bulk sample *per se* (for harder mortars or mortars perhaps with light pulverization) in multiple fresh batches of (1+3) HCl at ambient temperature. The former usually gives better result due to small amount, pulverization to easily remove the binder fraction for digestion, and use of rapidly heated acid, whereas latter method requires multiple episodes of digestion in fresh acid and is time-consuming. Acid digestion is also done as the first step to determine soluble silica content in a sample as described below, which is contributed from the hydraulic components in binder.

All these goals of acid digestion depend on the assumptions that: (i) sand is siliceous in composition and does not contain any acid-soluble constituents (e.g., carbonates), and, (ii) binder entirely dissolves in acid and does not contain any acid-insoluble constituents (gypsum, clay, etc.). Applicability of acid digestion to assess these tasks should therefore be first verified by optical microscopy to confirm the siliceous nature of sand without any appreciable acid-soluble constituents, and calcareous nature of binder, and none without any appreciable argillaceous (clay) constituents.

For grain-size distribution of sand (for sample found from optical microscopy to contain siliceous sand), a few representative fragments of (preferably not pulverized or lightly pulverized in a porcelain mortar and pestle for harder mortars to break down to smaller size fraction without crushing the sand to retain the original sand size) are selected for digestion in multiple fresh batches of (1+3) dilute hydrochloric acid to dissolve away all binder fractions and extract, wash, and oven-dry the acid-insoluble component of aggregate. Usually multiple episodes of acid digestion in fresh batches of acid and filtration of residues are needed to entirely remove the binder fractions without losing the finer fractions of sand. Sand particles thus extracted are washed, oven-dried, and sieved in an automatic mini sieve shaker through various U.S. Sieves from No. 4 (4.75 mm) through 8 (2.36 mm), 16 (1.18 mm), 30 (0.6 mm), 50 (0.3 mm), 100 (0.15 mm), and 200 (0.075 mm) for determination of the size, shape, angularity, and color of sands retained on various sieves. Grain-size distribution of sand is then compared with ASTM C 144 specifications for masonry sand. Photomicrographs of sand retained on each sieve are then taken with a stereomicroscope to record the sand size, shape, and color variations. For low amount of sample, or, for sample having calcareous sand, image analysis (e.g., ImageJ) on stitched photomicrographs of thin sections taken from multiple areas can be done to determine the sand-size distribution (Elsen et al. 2011).

## Cold Acid & Hot Alkali Digestion

Digestion of a pulverized sample of mortar in a cold acid followed by further digestion of residue in a hot alkali hydroxide solution are done to determine the soluble silica content contributed from the hydraulic component of binder, where cold acid digestion usually dissolves most of the binder without affecting the sand, followed by hot alkali hydroxide digestion to dissolve remaining soluble silica from calcium silicate hydrate component of paste or in mortars containing hydraulic binders. The soluble silica content corresponds to the silica mostly contributed from the hydraulic binder components (and a minor amount from any soluble silica component in the aggregates).

For determination of soluble silica content (modified from ASTM C 1324), 5.00 grams of pulverized sample (finer than 0.3 mm size, without excessive fines) is first digested in 100-mL cold (at 3 to 5°C) HCl and filtered through two 2.5-micron filter papers (filtrate #1). The residue with filter papers is then digested again in hot (below boiling) 75-ml NaOH, and filtered through two 2.5-micron filter papers (filtrate #2). The two filtrates from acid and alkali digestions are then combined, re-filtered twice with 2.5-micron and then through 0.45-micron filter paper to remove any suspended silica fines, brought to 250 ml volume with distilled water, and then used for soluble silica determination by an analytical method, such as atomic absorption spectroscopy (AAS), inductive coupled plasma optical emission spectroscopy (ICP-OES), or X-ray fluorescence spectroscopy (XRF). Multiple steps of filtrations from

2.5-micron to submicron filter papers are necessary to remove any suspended silica from sand that can skew the result. Instrument to be used for such determination must be calibrated with several silica standards in matrices similar to the one used in mortar analysis. An XRF unit calibrated with filtrates from acid-and-alkali-digested series of laboratory-prepared standards of Portland cement and silica sand mortars (moist cured at *w/c* of 0.50 for 30 days) having various proportions of Portland cements ($SiO_2$ contents of standards ranging from 1 to 10%) were used for determining $SiO_2$ Kα X-ray intensities from known stoichiometric silica (cement) contents of standards (using exact 5.00 grams as samples) prepared by the same procedure of cold HCl-digestion/filtration/hot NaOH-digestion/2$^{nd}$ filtration/combination of two filtrates/re-filtration steps as followed for mortars or mortars.

One of the standards used for calibration of XRF was re-used as an internal standard as the first sample during analyses of unknown sample. The standard Portland cement-silica sand mortar contained silica sand (finer than 0.3 mmm size) and 20 percent Portland cement (having 20.2% $SiO_2$). This standard mortar has a stoichiometric 4.04% soluble $SiO_2$ (i.e. equivalent to 0.202 gram or 202 mg $SiO_2$ in 250 ml filtrate of 5.00 grams of standard) to verify the accuracy of XRF results.

Soluble silica ($SiO_2$) content of sample in weight percent = A/B, where A = [*correction factor for standard*, which is 202 / (mg-$SiO_2$ of standard in 250 ml filtrate from XRF)] × [*ppm-$SiO_2$ of sample*, which is 4 (for 250 ml to 1L for ppm) × (mg-$SiO_2$ of sample in 250 ml filtrate from XRF)] × [*filtrate volume in ml used without dilution*, which is 250]; and B = [*Sample weight in grams*, which is 5.00] × [*ppm to wt.% conversion*, which is 10,000]. Recovery of soluble silica in standard after cold-HCl/hot-NaOH digestion is usually 180 to 200 mg. in 250 ml filtrate in XRF (i.e. correction factor of 1.0 to 1.2).

Hydraulic binder content is then calculated as: [(soluble $SiO_2$, weight percent in sample as calculated above) divided by assumed soluble $SiO_2$ content in binder] ×100, where assumed $SiO_2$ contents of binders varies with binder types, e.g., 21% in Portland cement, 20% in natural cement, 27% in slag cement, 7 to 10% in hydraulic lime, etc., or, more preferably, from the average paste-$SiO_2$ content determined from SEM-EDS.

## Weight Losses on Ignition

Losses in weight of a mortar on step-wise heating from ambient to 110°C, 550°C, and 950°C temperatures liberate free water from capillary pore spaces by 110°C, combined water from dehydroxylation of various hydrous phases (calcium silicate hydrate, calcium hydroxide, etc.) by 550°C, and liberation of carbon dioxide from decomposition of carbonated paste and carbonate minerals by 950°C. Such losses in weight are measured by following the procedures of ASTM C 1324 by heating 1.00 gram of pulverized mortar (finer than 0.3 mm) in an alumina crucible in a muffle furnace in a controlled step-wise heating at a heating rate of 10ºC/min. Mortars having hydraulic binders and hydration products of such provide measurable combined water contents after calcination to 550°C, whereas those having high calcareous components (high-calcium lime mortar or mortar having calcareous sand) produce higher weight losses during ignition to 950°C. Usually, a good correlation is found between weight losses at 550°C from dehydration of combined water, and, soluble silica contents contributed from hydraulic binders amongst series of mortars containing variable amounts of hydraulic phases.

## X-ray Diffraction (XRD)

X-ray diffraction (XRD) is useful for: (a) determination of bulk mineralogical composition of mortar, including its aggregate and binder mineralogies (e.g., quartz in sand from major diffraction peaks at 26.65º, 20.85º, 50.14º 2θ, or calcite in sand or carbonated lime binder from major peaks at 29.41º, 39.40º, 43.15º 2θ, or Portlandite in binder from major peaks at 34.09º, 18.09º, 47.12º 2θ); (b) individual primary mineralogies and alteration products of aggregates at various size fractions, and binder phases; (c) detection of dolomitic lime binder from brucite in the sample from major peaks at 38.02º, 18.59º, 50.86º 2θ; (d) detection of use of lime (portlandite), gypsum (11.59º, 20.72º, 29.11º 2θ), or cement binders from their characteristic mineralogies; (e) detection of any potentially

deleterious constituents, e.g., deleterious salts, or efflorescence deposits; (f) detection of a mineral oxide-based pigment in sample; and (g) detection of components difficult to detect by microscopical methods.

X-ray diffraction can be done on: (i) pulverized (to finer than 45 micron) portion of bulk sample, or (ii) on the sand extracted from mortar by acid digestion, if sand has a complex mineralogy, or also (iii) on the binder-fraction by separating sand from the binder from a carefully ground sample (in a mortar and pestle) and passing the ground mass through US 200 sieve (75 micron) to collect the fraction rich in binder. XRD pattern of a sample containing silica sand typically shows quartz as the dominant phase that surpasses peaks for all other phases (e.g., calcite, dolomite, clay, secondary deposits); hence binder separation is sometimes useful to detect minor minerals of interest (e.g., salts or pigments). For mortars containing marine shell fragments as sand, aragonite appears with calcite as two calcium carbonate phases from the shell fragments and paste. For binder mineralogy, sample is first dried at 40°C to a constant mass, then carefully crushed without pulverizing the sand, and sieved through a 75-micron opening screen to retain sand-rich fraction on the sieve and obtain the passed binder-rich fraction for further pulverization down to finer than 45 micron. Salts and other soft components can be analyzed from binder fraction. Efflorescence salts on masonry walls are also analyzed routinely in XRD.

For sample preparation, a Rocklab (Sepor Mini-Thor Ring) pulverizer is used to grind sample down to finer than 100 microns. Usually, a few drops of anhydrous alcohol are added to reduce decomposition of hydrous phases from the heat generated from grinding. Approximately 10 grams of sample is ground first in the pulverizer, from which about 8.0 grams of sample is selected, mixed with an appropriate binder (e.g., three Herzog grinding aid pellets from Oxford Instruments having a total binder weight of 0.6 gram for 8 grams of sample for a fixed binder proportion of 7.5 percent); the mixture is then further ground in Rocklab pulverizer and in a McCrone micronizing mill with anhydrous alcohol down to finer than 44 micron size. Approximately 7.0 grams of binder-mixed pulverized sample thus prepared is weighed into an aluminum sample cup and inserted in a stainless steel die press to prepare the sample pellet. A 25-ton Spex X-press is used to prepare 32 mm diameter pellet from the pulverized sample. The pressed pellet is then placed in a custom-made circular sample holder for XRD and excited with the copper radiation of 1.54 angstroms. Sample holders made with quartz or silicon are best for working with very small quantities of sample because these holders create no diffraction peaks between 2° and 90° 2θ (Middendorf et al. 2005).

XRD is carried out in a Siemens D5000 Powder diffractometer (θ-2θ goniometer) employing a long line focus Cu X-ray tube, divergent and anti-scatter slits fixed at 1 mm, a receiving slit (0.6 mm), diffracted and incident beam Soller slits (0.04 rad), a curved graphite diffracted beam monochromator, and a sealed proportional counter. Siemens D 5000 is equipped with (a) a horizontal stage (fixed), (b) an X-ray generator with CuKα, fine focus sealed tube source, (c) large diameter goniometer (600 mm), low divergence collimator, and Soller slits, (d) fixed detector slits 0.05, 0.2, 0.6, 1.0, 2.0, and 6.0, and (e) Scintillation detector. Generator settings used are 40 kV and 30 mA. Tests are usually run at 2θ from 4° to 64° with a step scan of 0.02° and a dwell time of one second. The resulting diffraction patterns are collected by DataScan 4 software of Materials Data, Inc. (MDI), analyzed by Jade software of MDI with ICDD PDF-4 (Minerals 2017) diffraction data. Phase identification, and quantitative analyses were carried out with MDI's Search/Match, Easy Quant, and Rietveld modules, respectively.

## X-ray Fluorescence (XRF)

X-ray fluorescence (XRF) is used for determining: (a) major element oxide composition of sample, and, (b) soluble silica content of filtrate after digestion of sample in cold-HCl and hot-NaOH. Major element oxide compositions provide clues about the siliceous sand content of mortar from silica content, type of binder used (e.g., a dolomitic lime or natural cement based binder gives a characteristically higher magnesia than a calcitic lime or Portland cement based binder), calculation of lime content in a cement-lime mortar from bulk CaO content from XRF, effect of alterations and deteriorations (e.g., salt ingress in a mortar from marine environment can be diagnosed from excessive sodium, sulfate, and chlorine, etc.), etc. A series of standards from Portland cements, lime, gypsum, to various rocks, and masonry cements of certified compositions (e.g., from USGS, GSA, NIST, CCRL, Brammer, or measured by ICP) are used to calibrate the instrument for various oxides, and empirical calculations are done from such calibrations to determine oxide compositions of mortars. For mortars with highly unusual compositions (e.g.

severely salt-contaminated or a gypsum-based mortar) a standard-less FP calculation is done to determine the best possible composition.

An energy-dispersive bench-top X-ray fluorescence unit from Rigaku Americas Corporation (NEX-CG) was used. Rigaku NEX-CG delivers rapid qualitative and quantitative determination of major and minor atomic elements in a wide variety of sample types with minimal standards. Unlike conventional EDXRF analyzers, the NEX-CG was engineered with a unique close-coupled Cartesian Geometry (CG) optical kernel that dramatically increases signal-to-noise. By using monochromatic secondary target excitation, instead of conventional direct excitation, sensitivity is further improved. The resulting dramatic reduction in background noise, and simultaneous increase in element peaks result in a spectrometer capable of routine trace element analysis even in difficult sample types. The instrument is calibrated by using various certified (CCRL, NIST, GSA, and Brammer) reference standards of cements and rocks. The same pressed pellet used for XRD for mineralogical compositions is used for XRF to determine the chemical composition.

## Thermal Analyses (TGA, DTG, and DSC)

Thermal analyses encompass: (1) thermogravimetric analysis (TGA), which measures the weight loss in a sample as it is heated, where weight loss can be related to specific physical decomposition of a phase of interest at a specific temperature that is characteristic of the phase from which both the phase composition and the abundance can be determined; (2) differential thermal analysis (DTA, or first derivative of TGA i.e. DTG) measuring temperature difference between the sample and an inert standard ($Al_2O_3$) both are heated at the same rate and time where endothermic peaks are recorded when the standard continues to increase in temperature during heating but the sample does not due to decompositions (e.g., dehydration of hydrous or decarbonation of carbonate phases); the endothermic or exothermic transitions are characteristic of particular phase, which can be identified and quantified using DTA (or DTG); and (3) differential scanning calorimetry (DSC), which follows the same basic principle as DTA, whereas temperature differences are measured in DTA, during heating using DSC energy is added to maintain the sample and the reference material ($Al_2O_3$) at the same temperature; this energy use is recorded and used as a measure of the calorific value of the thermal transitions that the sample experiences; this is useful for detection of quartz that undergoes polymorphic (α to β form) transitions and no weight loss.

Thermal analyses are done to determine the presence and quantitative amounts of: (a) hydrates (e.g., combined water liberated from paste dehydration during decomposition of calcium-silicate-hydrate component in paste at 180-190ºC); (b) sulfates (gypsum from decompositions at 125ºC, and 185-200ºC, ettringite at 120-130ºC, thaumasite at 150ºC); (c) brucite from its dehydroxylation at 300-400ºC to confirm the presence of dolomitic lime; (d) hydrate water from decomposition of Portlandite component of paste at 400-600ºC; (e) quartz from polymorphic transformation (α to β form) at 573ºC; (f) cryptocrystalline calcite in the carbonated lime matrix from decomposition at 620-690ºC, or magnesite at 450-520ºC, or (g) coarsely crystalline calcite e.g., in limestone by decomposition at 680-800ºC or (h) dolomite at 740-800ºC and 925ºC, and (i) phase transition of belite ($C_2S$) at 693ºC, etc. Phases are determined from their characteristic decomposition temperatures occurring mostly as endothermic peaks or polymorphic transition temperatures as for quartz.

Simultaneous TGA and DSC analyses were done in a Mettler Toledo TGA/DSC 1 unit on 30-70 mg of finely ground (<0.6 mm) sample in alumina crucible (70 µl, no lid) from 30°C to 1000°C at a heating rate of 10°C/min with high purity nitrogen as purge gas at a flow rate of 75.0 ml/min. TGA/DSC 1 simultaneously measures heat flow in addition to weight change. The instrument offers high resolution (ultra-microgram resolution over the whole measurement range), efficient automation (with a reliable sample robot for high sample throughput), wide measurement range (measure small and large sample masses and volumes) broad temperature scale (analyze samples from ambient to 1100°C), superior ultra-micro balance, simultaneous DSC heat flow measurement (for simultaneous detection of thermal events, e.g., polymorphic alpha-to-beta transition of quartz and quartz content), and a gastight cell (ensures a properly defined measurement environment).

## Fourier Transform Infra-red Spectroscopy (FT-IR)

Fourier-transform infrared spectroscopy (FT-IR) measures interaction between applied infrared radiation and the molecules in the compounds of interest (Middendorf et al. 2005). FT-IR is particularly useful for detection of admixture, additives, and polymer resins, mainly to identify various organic components (functional groups) in mortar (e.g., methyl $CH_3$, organic acids CO-OH, carbonates $CO_3$) from their characteristic spectral fingerprints in FT-IR spectrum. FT-IR can also be used for detection of main mineral phases in a hydraulic binder, CSH, carbonates, gypsum, and clays (Middendorf et al. 2005). Organic compounds such as synthetic (e.g., acrylics, polyesters) and natural resins, carbohydrates, colorants, oils and fats, proteins, waxes as well as inorganic compounds, e.g., corrosion products, minerals, pigments, paints, fillers, stone, glass, and ceramics can be detected by this technique.

FT-IR measurements are done in a Perkin Elmer Spectrum 100 FT-IR spectrophotometer running with Spectrum 10 software. Sample is measured using attenuated total reflection (ATR) on a single bounce diamond/ZnSe ATR crystal between a frequency range of 4000 to 650 $cm^{-1}$. Each run is collected at 4 $cm^{-1}$ resolution with Strong Beer-Norton apodization. Data are collected with a temperature-stabilized deuterated triglycine sulfate (DTGS) detector by placing the sample in contact with the ATR crystal and by applying force from the pressure applicator supplied with the ATR accessory. The application of pressure enable the sample to be in intimate contact with the ATR crystal, ensuring achievement of a high-quality spectrum. Additionally, more conventional KBr pellet is also sometimes used for samples on as-needed basis.

## Ion Chromatography

Salts can cause various deteriorations from: (a) mere aesthetic issues of surface efflorescence by precipitation from evaporation of leachates on the surfaces followed by atmospheric carbonation of the precipitates where salts deposit as individual crystals or as crust to (b) more serious internal distress in mortar from crystallization inside the pores (sub-fluorescence or crypto-fluorescence) from expansive forces associated with crystallization of salt from supersaturated solutions. Some common salts are calcium carbonates (e.g., calcite, vaterite), magnesium carbonate (magnesite), sodium carbonate hydrate and bicarbonate (thermonatrite, trona, nahcolite), sulphates (gypsum, thenardite, epsomite, melanterite, mirabilite, glauberite, or ettringite and thaumasite from oxidation of sulfides or cement hydrates), and chlorides (halite, sylvite, calcium oxychloride from deicing salts, salt-bearing aggregates, ground water). X-ray diffraction and SEM-EDS can determine many of these salts as long as they are present in detectable amounts. Ion chromatography is an established technique used for analyses of various water-soluble anions and cations in salts (e.g., chloride, sulfate, and nitrate anions, and magnesium, calcium, alkali, ammonium cations) to assess magnitude of environmental impacts on masonry units and mortars, and subsequent effects of such salt ingress. Samples are pulverized, digested in deionized water to remove all water-soluble salts, then solid residues are filtered out and the water-digested filtrates are analyzed by an ion chromatograph.

Ion chromatography methods are described in ASTM D 4327 “Standard Test Method for Anions in Water by Chemically Suppressed Ion Chromatography.” Briefly, an aliquot of 1 gram of pulverized sample (passing No. 50 sieve) was digested in 50 ml distilled water for 6 to 8 hours on a magnetic stirrer at a temperature below boiling point of water; then the digested sample was filtered through two 2.5-micron filter papers using vacuum, followed by a second filtration through micro-filter (0.45 micron) paper, then the filtrate was either used directly or diluted to 100 to 250 ml with distilled water depending on the concentration of anions, and used for analysis to get ppm-level fluoride, chloride, nitrite, bromide, nitrate, phosphate, and sulfate in the water-digested sample in Metrohm 861 Advanced Compact IC. The instrument was calibrated against six different custom-made Metrohm anion standard solutions having all these anions from 0.1-ppm to 100-ppm levels. To check the accuracy of the instrument, a 50-ppm standard solution was run first prior to the analyses of samples.

**Laboratory Analyses of Masonry Mortars**

Initial Mortar (50 to 100 grams) [Photographed with digital camera & flat-bed scanner, As-received condition, total weight, and dimensions of largest piece are documented]

Intact Pieces (20+ g)

***1. Optical Microscopy***

I. Perform visual examination of mortar as received, then saw-cut and fractured surfaces and with a low-power stereomicroscope,
II. Take digital and flat bed scanner photos of intact piece(s),
III. Encapsulate the piece for thin section microscopy in a flexible mold with a low-viscosity colored or fluorescent dye-mixed epoxy to highlight voids, pores, cracks, etc.,
IV. Prepare thin section (< 30 micron thickness) and polish the thin section for optical and SEM-EDS analyses,
V. Scan the thin section on a flat-bed scanner with the thin section residue,
VI. Take transmitted light high-power stereo-zoom photomicrographs of thin sections from different areas to be stitched to determine volumes and size distributions of pore spaces and sand grains by Image J,
VII. Take plane and crossed polarized-light photomicrographs of sand and binder fractions in thin section from a petrographic microscope and determine areas for further studies by SEM-EDS,
VIII. Do detailed petrographic examinations to determine the sand and binder compositions, sand mineralogy and texture, binder phases, residual binders, alterations, and products of any deleterious reactions, immersion mounts of specific areas of interest, etc.

***2. SEM-EDS***

I. Put conductive coating only on the portion of polished thin section intended for SEM-EDS studies from optical microscopy,
II. Take backscatter and/or secondary electron images, and if needed X-ray elemental maps,
III. Select multiple areas on paste to determine oxide compositions and Eckel's cementation indices,
IV. Tabulate the paste composition variations across the backscatter/secondary electron image.
V. Determine chemical compositions of resides left from the original components of the binders, as well as the hydration and carbonation and other alteration products

Lightly hand-ground in a Mortar & Pestle (30+ g)

***3. Acid Digestion - Sand Color & Sand Size Distribution*** (10 g)

I. Take 10 g. of mortar lightly ground in mortar & pestle and digest in HCl (1+3) in a 250 ml beaker on a magnetic stirrer until all sand separates and settles at the bottom of beaker,
II. Filter all through two 2.5 micron filter paper, wash the beaker, filter paper, and all sand residue with dist. water,
III. Dry the residue at 110°C in an oven for 10 min., gently brush out from the filter paper and collect, then sieve the entire sand residue through No. 4 through 200 sieves in a mini sieve shaker (e.g., from Gilson),
IV. Determine the mass retained on each sieve, and on the pan (finer than No. 200 sieve),
V. Take photomicrographs of sand particles retained on each sieve for sand color variations in a stereomicroscope.

***4. Acid & Alkali Digestion – Soluble Silica for Hydraulic Binder*** (5 g)

I. Grind 5-6 g of lightly ground fraction from mortar & pestle in a WC pulverizer for 30 sec.
II. Sieve thru. No. 50 sieve, collect the fraction passing the sieve,
III. Re-grind the residue retained on sieve for 15 sec. and mix thoroughly with the previous fraction;
IV. Use 5.000 g of thus prepared powder (passing No. 50 sieve) for digestion in 100 ml cold (3-5°C/38-41°F) HCl (1+4) in a 250 ml beaker for 15 min. on a magnetic stirrer,
V. Filter thru. two 2.5 micron filter paper and keep the filtrate# 1,
VI. Digest the residue with filter paper in 75 ml hot NaOH (below boiling) on hot plate for 15 min. on magnetic stirrer,
VII. Cool down to room temp. and filter thru. two 2.5 micron filter paper and collect filtrate# 2,
VIII. Combine these two filtrates, filter the combined filtrates thru. two 2.5 micron filter paper to remove any suspended silica (especially for sand-rich mortars, or if mortar is grounded too long); then dilute to 250 ml in a volumetric flask with dist. water, an aliquot (about 10 ml) is then used for XRF for soluble silica determination against the calibrations with standard PC mortars of known soluble silica contents prepared in the same way.

***5. Acid Digestion – Acid-Insoluble Residue Content for Siliceous Sand Content*** (2 g)

I. Take 1-2 g of prepared mortar powder from Step 4 iii (passing No. 50 sieve) and digest in 50 ml HCl (1+3) in a 250 ml beaker (covered) on a hot pate rapidly near boiling, then 15 min. at a temp. below boiling, then cool down to room temperatures,
II. Filter thru. two pre-weighed 2.5 micron filter papers, washing the beaker, paper, and residue thoroughly with hot water,
III. Dry the filter paper at 110C for 10 min, cool in a desiccator to room temp. and measure the weight.
IV. Subtract from mass of dry filter paper to determine acid-insoluble residue content.

***6. Chemical Analysis – Loss On Ignition for Free and Combined Water Content, and Carbonate plus Carbonation*** (2 g)

I. Take 1-2 g ($W_1$) of prepared mortar powder from Step 3 iii (passing No. 50 sieve) in a tarred porcelain crucible (keep a record of mass of the empty crucible),
II. Dry at 110°C for 15 min in a muffle furnace pre-set to 110°C, cool in a desiccator to room temp. and measure the mass ($W_2$) by subtracting the empty crucible mass from the total mass,
III. Ignite at 550°C for 15 min. in the muffle furnace pre-set to 550°C, cool in a desiccator to room temp. and measure the mass ($W_3$) by subtracting the empty crucible mass from the total mass,
IV. Ignite at 950°C for 15 min. in the muffle furnace pre-set to 950°C, cool in a desiccator to room temp. and measure the mass ($W_4$) by subtracting the empty crucible mass from the total mass,
V. Calculate the losses on ignition at 110°C, 550°C, and 950°C for free water, combined water, and carbonate plus degree of carbonation, respectively.

***7. Mineralogy of Bulk Mortar, Extracted Sand, Extracted Binder, or Salt from XRD*** (at least 8 g)

I. Weigh 8.00 g of mortar (or extracted sand or binder as needed) lightly ground in a mortar & pestle, add three grinding/pelletizing aid tablets (e.g., from Oxford Instruments) and pulverize in a suitable mill to minimize contamination (e.g., Rocklab pulverizer with WC bowl or McCrone Micronizing Mill with agate) for 3 min. with anhydrous alcohol to get <45 micron size particles passing U.S. No. 325 sieve,
II. Take 6.8 to 7.0 g. of ground <45 micron prepared mass in an aluminum sample holder inside a stainless steel die to prepare a 32 mm pellet with 25 ton pressure for 1 min,
III. Use the prepared pellet for XRD and then use the same pellet for XRF.
IV. Do XRD on the binder-rich fraction, or salt either on a shallow-depth sample holder or preferably on a zero background quartz plate for small volume of sample.

***8. Bulk Mortar's Composition from X-Ray Fluorescence (XRF)*** (same pellet used in XRD)

I. Use the same pellet prepared for XRD in the XRF, or, use a fused bead if sample volume is low to prepare a pellet. In either method, have calibrations of measured oxides with adequate standard.
II. XRF can also be used with proper calibrations for soluble silica determination on the filtrates after acid and alkali digestions, as described in Section 4.

***9. Thermal Analyses*** (0.1 g), TGA, DTG, DSC, DTA, for quantitative analysis of various hydrous, sulfate, and carbonate phases in mortar, content of dolomitic lime added from the brucite content in mortar as determined from TGA or DSC, etc.

I. Simultaneous TGA and DSC analyses can be done on 30-70 mg of finely ground (<0.6 mm) mortar in alumina crucible (70 µl, no lid) from 30°C to 1000°C at a heating rate of 10°C/min with high purity nitrogen as purge gas at a flow rate of 75.0 ml/min .

***10. Infrared Spectroscopy,*** for determination of various organic additives, paint, and clays in mortar

I. Take an aliquot of powder prepared for thermal analysis, or peel a paint and use that in Universal ATR of FTIR.
II. Alternately, digest a pulverized mortar in acetone to extract the organic additive and analyze the liquid in FTIR for characteristic functional groups.

***11. Ion Chromatography of Water-Soluble Salts*** (1 g)

I. Take an aliquot of 1.00 gram powder prepared for chemical analysis (i.e. passing U.S. No. 50 sieve), digest in hot (below boiling) 50 ml distilled or deionized water for at least 6 hours in a beaker on a magnetic stirrer covered with watch glass, filter the solid residues out to collect the filtrate and analyze the final 100 ml of filtrate for soluble salts (chloride, sulfate, nitrate, nitrite, phosphate, etc.) by ion chromatography.

Figure 5: Outline of step-by-step procedures of various laboratory analyses of a masonry mortar. FTIR was not needed for the present mortar sample.

# RESULTS

## Grain-size Distribution of Sand

Figure 6 shows grain-size distribution of sand extracted after a series of digestion of representative mortar fragments in dilute (1+3) hydrochloric acid. Also shown are micrographs of sand particles taken with a stereomicroscope retained on various sieves including size, shape, angularity, and color variations of sand particles. Note noticeably darker gray color tone of majority of sand particles that are mostly rounded to sub rounded argillaceous particles mixed with a subordinate amount of off-white to light gray siliceous grains. A few particles retained on Nos. 50 and 100 are still agglomerated due to incomplete separation of binder from sand despite repeated acid digestion. It is important to remember that many soft argillaceous sand particles may have broken down during acid digestion and calcareous particles, if present, are mostly dissolved out in acid. Hence, photos of particles retained on each sieve are mostly from the sound argillaceous and siliceous component of sand.

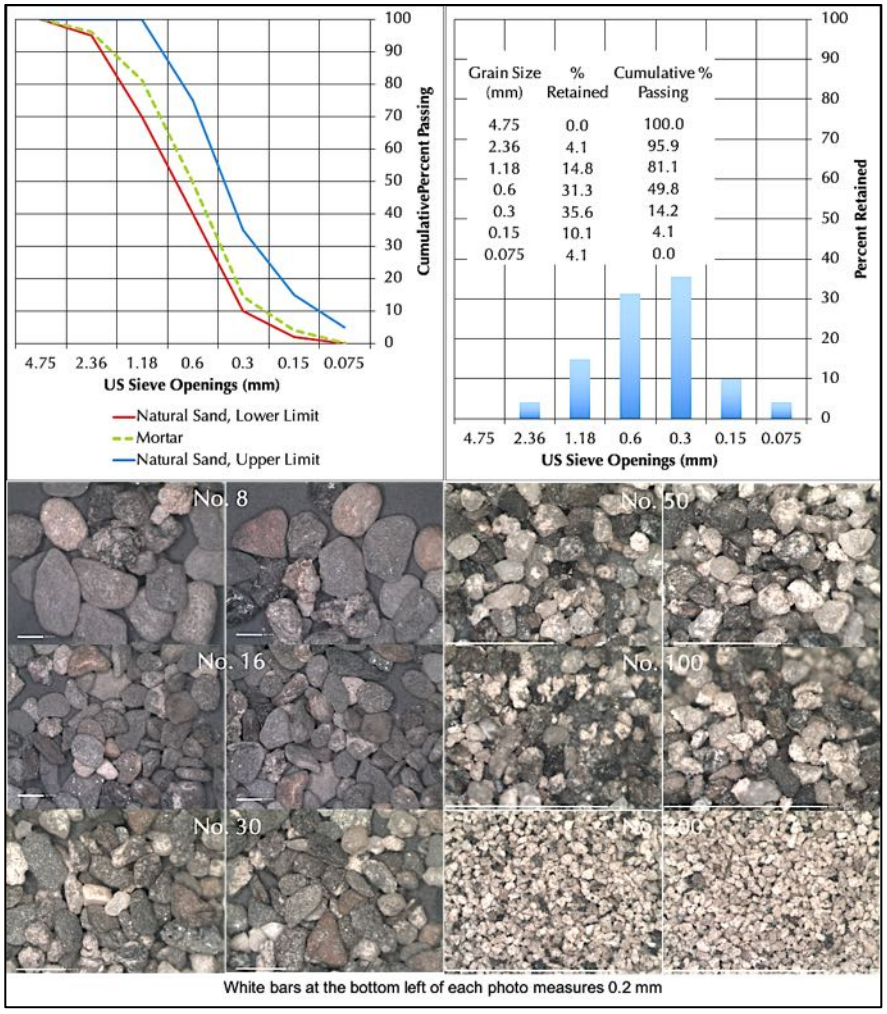


Figure 6: Grain-size distribution of sand extracted from the mortar after acid digestion. In the top left plot, size distirbution of sand is compared with upper and lower limits of natural sand in ASTM C 144 (blue and red lines). Top right plot shows normal distribution of sand. Bottom photos show stereo-photomicrographs of sand particles retained on various sieves.

Size distribution of sand in the mortar is compared with the ASTM C 144 specification of natural sand for unit masonry, which shows that for all size fractions, sand is within (in conformance to) the upper and lower limits of ASTM C 144 size gradation for natural sand. The 'percent retained' histogram plot shows 'normal' size distribution of sand without any enrichment of fines. Therefore, sand is judged to be overall similar to a modern ASTM C 144 masonry sand in terms of grain-size distribution.

Subsequent optical microscopical examinations of sand determined its **argillaceous-siliceous composition where the dark gray color tone of sand is from argillaceous and ferruginous particles in sand**, and lack of any calcareous components. Therefore, sand extracted from acid digestion is determined to be the entire amount of sand without leaving any component and hence results provided here are representative of the bulk sand used.

## Optical Microscopy of Sand

Figure 7 shows micrographs of saw-cut cross section of mortar taken with a reflected-light Stereozoom microscope to show the overall size, shape, distribution, gradation, and composition of sand in the mortar, as well as color and appearance of interstitial binder, and air voids. Sand particles are less than 2 mm in nominal size (consistent with >95 percent particles passing through 2.36-mm sieve openings in Figure 6), subangular to subrounded to well-rounded, mostly equidimensional to a few elongated in shape, and appear in color ranges from colorless to dark gray to reddish-brown, as seen in the photos. Rounded to subrounded shapes of most sand particles are indicative of use of a natural sand (from a river sand source). Interstitial paste is characteristically brown with no evidence of use of any air-entraining agent, consistent with its historic nature.

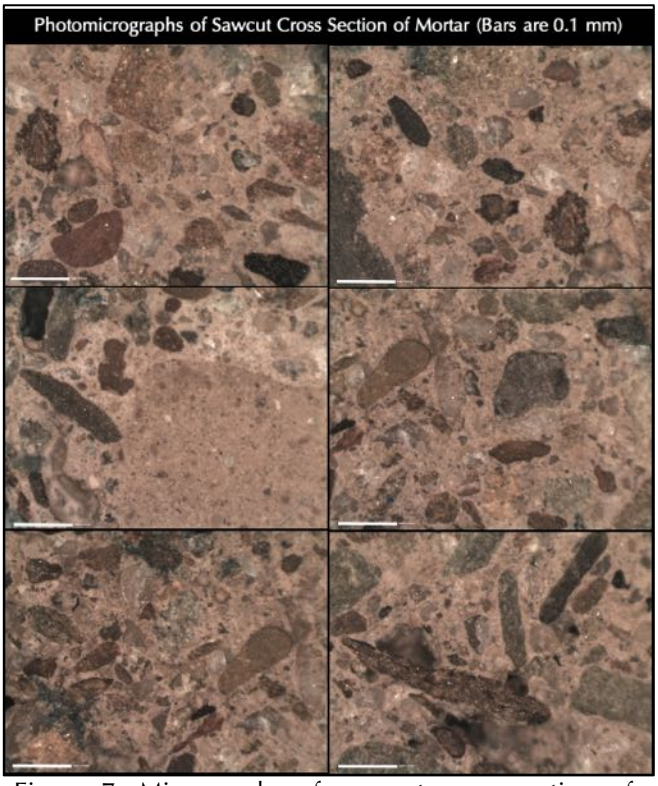


Figure 7: Micrographs of saw-cut cross section of mortar.

Figures 8 and 9 show crossed (right column) and corresponding plane (left column) polarized-light views of micrographs of the blue dye-mixed epoxy-impregnated thin section of mortar (Figure 4) viewed in a transmitted-light Stereozoom microscope. Sand particles show mixed argillaceous (shale), siltstone, and ferruginous particles and single and multi-crystal quartz, quartzite, feldspar, schist, and other siliceous composition of natural sand. No calcareous component is found. Almost half of the sand particles are constituted of argillaceous and ferruginous particles.

The plane-polarized light photos in Figure 8 show irregular-shaped interstitial voids with an appearance of a **non-air-entrained mortar** where voids are highlighted by blue epoxy. Such non-air-entrained nature is characteristic of many historic masonry cement mortars from the late 19$^{th}$ century.

Interstitial matrix between sand particles shows ultrafine-grained, severely carbonated lime and natural cement composition of paste having a few, sporadic residual natural cement particles in paste that shows carbonate mineralogy and microstructure of argillaceous dolomitic limestone raw feed used in production of natural cement, carbonated patches of lime, etc., all of which are characteristic features of a **lime and natural cement-based binder in the mortar** made using natural sand, lime putty, and natural cement binder as described later in the paste section.

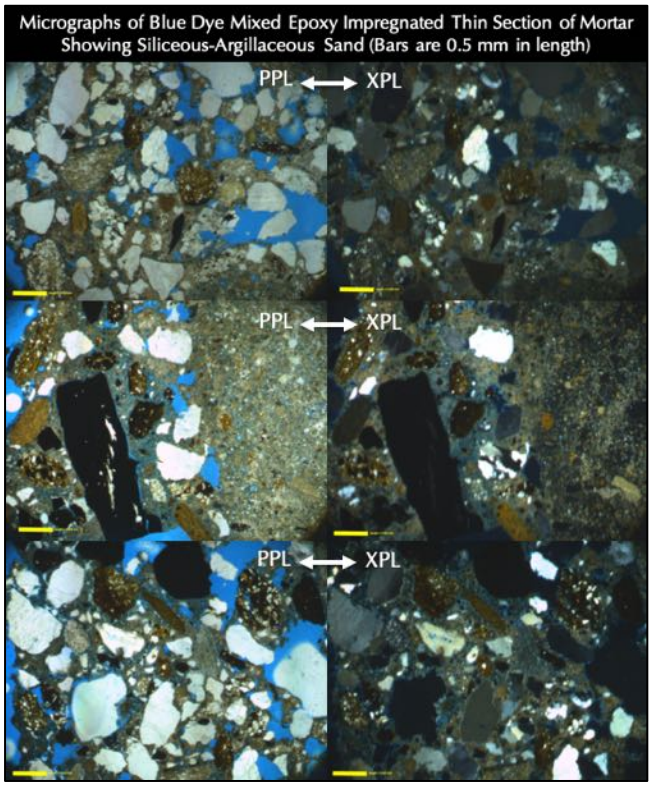


Figure 8: Micrographs of thin section of mortar taken with a transmitted-light Stereozoom microscope (bars are 0.5 mm in length).

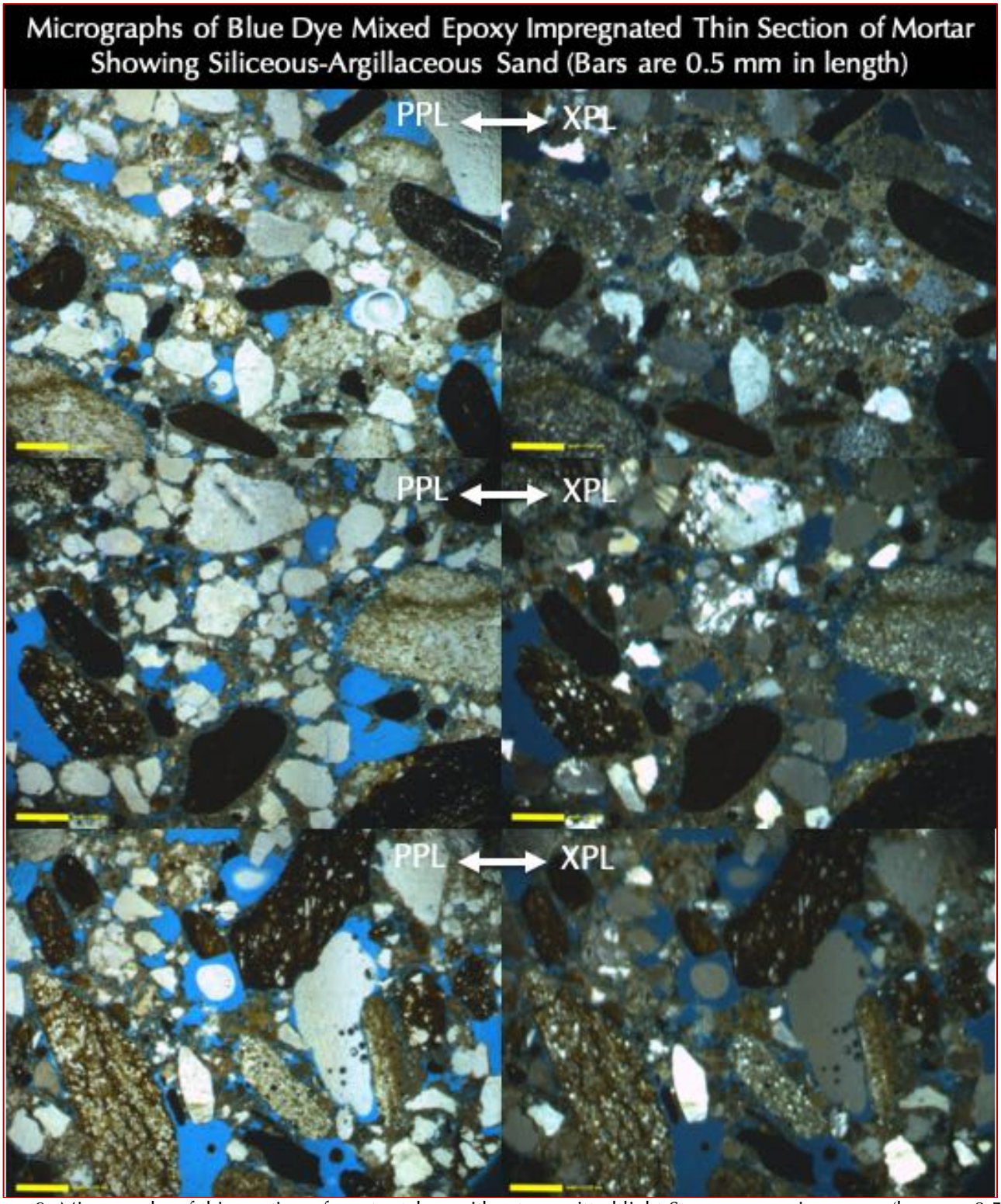


Figure 9: Micrographs of thin section of mortar taken with a transmitted-light Stereozoom microscope (bars are 0.5 mm in length) showing major amounts of argillaceous (shale), siltstone, and ferruginous particles, and single and multi-crystal quartz, quartzite, feldspar, schist, and other siliceous composition of natural sand. No calcareous component is found. Almost half of the sand particles are constituted of argillaceous and ferruginous particles.

Figure 10 shows black-and-white binary images of the left column of plane-polarized light photos in Figure 8 (shown in left) to highlight in black the void spaces and shrinkage microcracks in the middle column, and, sand particles in right column against everything else in white.

Image analyses of these binary images (by Image J, from the National Institute of Health, www.imagej.nih.gov) provide a *rough estimate* of 6.3 percent void spaces, which are mostly the interstitial and coarse voids, and, 29.8 percent sand by area.

Figure 11 shows micrographs of thin section of mortar from transmitted-light petrographic microscope in plane-polarized light (PPL) and corresponding crossed-polarized light (XPL) modes, which show detailed compositions and textures of individual sand particles. Observations in petrographic microscope confirmed the argillaceous-ferruginous-siliceous composition of sand and the presence of shale as the dominant argillaceous component and quartz as the dominant siliceous component of sand.

The siliceous quartz-quartzite component of sand particles are mostly angular as opposed to rounded and sub-rounded argillaceous (shale) and ferruginous particles indicting a crushed nature of siliceous sand, which was mixed with a river sand of dominantly argillaceous-ferruginous composition.

The siliceous sand particles are present in sound condition without any potentially deleterious reactions (e.g., alkali-aggregate reactions). The argillaceous and ferruginous components, however, are potentially unsound in the presence of moisture during service.

Based on these observations, sand for the mix for replacement mortar in renovation can be used from a local river sand source after conducting a petrographic examination of the sand to be used *a la* ASTM C 295 to confirm the match with the sand found in this examined mortar. Argillaceous and ferruginous components should preferably be avoided.

Intricate details in all optical micrographs in Figures 7 through 17 can be best viewed by enlarging these pages.

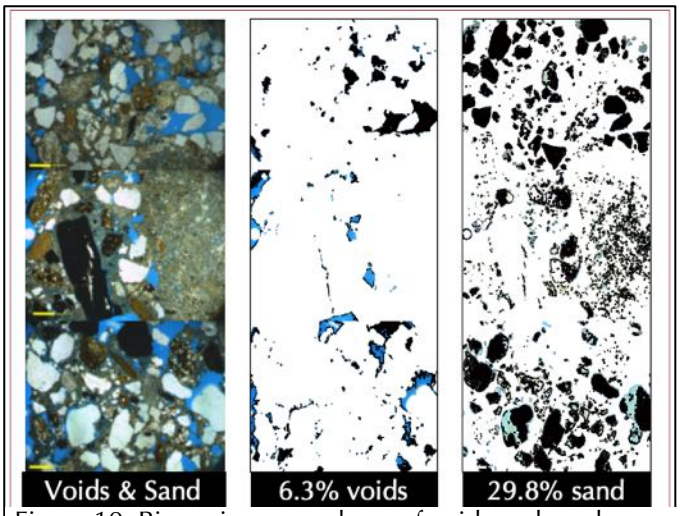

Figure 10: Binary image analyses of voids and sand.

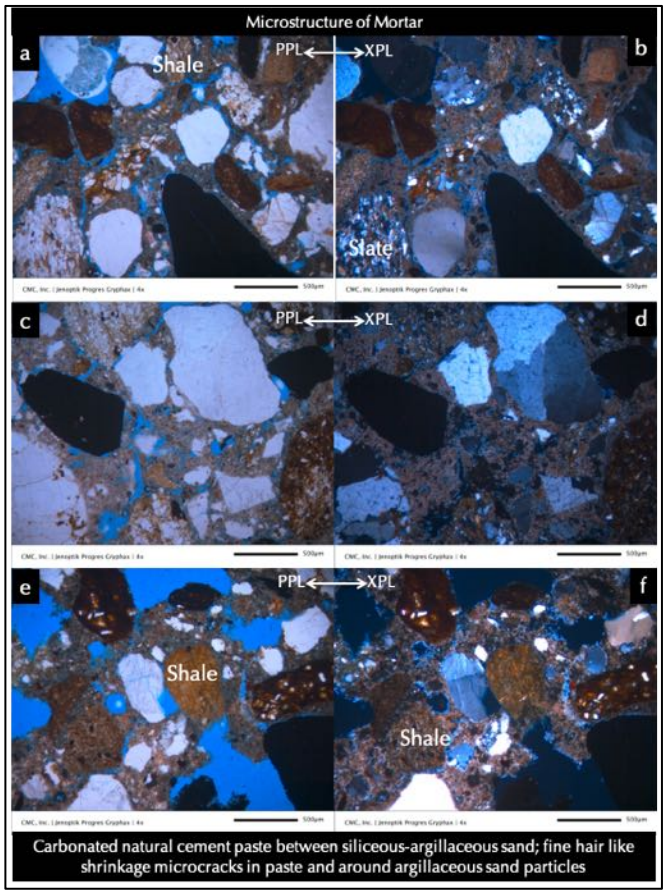

Figure 11: Mortar sand as seen through a petrographic microscope. Sand consists of mainly siliceous quartz, quartzite, and feldspar particles, mostly subangular to well-rounded, well-graded, and well-distributed.

## Optical Microscopy of Paste

Figures 12 and 13 provide micrographs of the interstitial matrix phases of paste between sand particles to characterize the compositions and microstructure of binder as revealed from micrographs of thin section of mortar in a petrographic microscope.

Figure 12 shows severely carbonated and leached, altered nature of the paste, which has features that are characteristic of many historic mortars where original binder components and their subsequent carbonation and hydration products are leached out, obliterated, and altered during centuries of service and interactions with the environment.

Figure 12 shows contrasting porosities and densities of paste between denser cement hydrated areas and more porous and carbonated lime-rich areas that are characteristic of lime and natural cement mortars. A few residual natural cement particles are boxed.

Figure 12 shows plane (left) and corresponding crossed (right) polarized light views of thin section images depicting a residual natural cement particle (arrows) having characteristic calcium-aluminate-silicate mineralogies and contrasting denser and porous leached paste areas.

Within the paste areas in Figures 12 and 13 are: (a) residual natural cement particles representing calcined residues of argillacoeus dolomitic limestone, (b) areas of cement hydration products, (c) isolated patches of carbonation of lime, (d) areas rich in porous and carbonated lime, and (e) severe leaching, alteration, carbonation of paste – all juxtaposed with interstitial voids – all carrying a tale-tell feature of a historic lime and natural cement based mortar.

Based on optical microscopy alone, therefore, the mortar is determined to have a lime, natural cement, and argillaceous-siliceous-ferruginous sand based composition made using natural cement and lime putty as the binder. The lime component was derived from calcination of relatively magnesian (or dolomitic) limestone, whereas natural cement component was derived from calcination of an impure (argillaceous) limestone feed similar to the ones used for the production of Rosendale cements.

Subsequent SEM-EDS studies of paste determined the dolomitic composition of lime and natural cement component in the binder from high magnesia contents of paste.

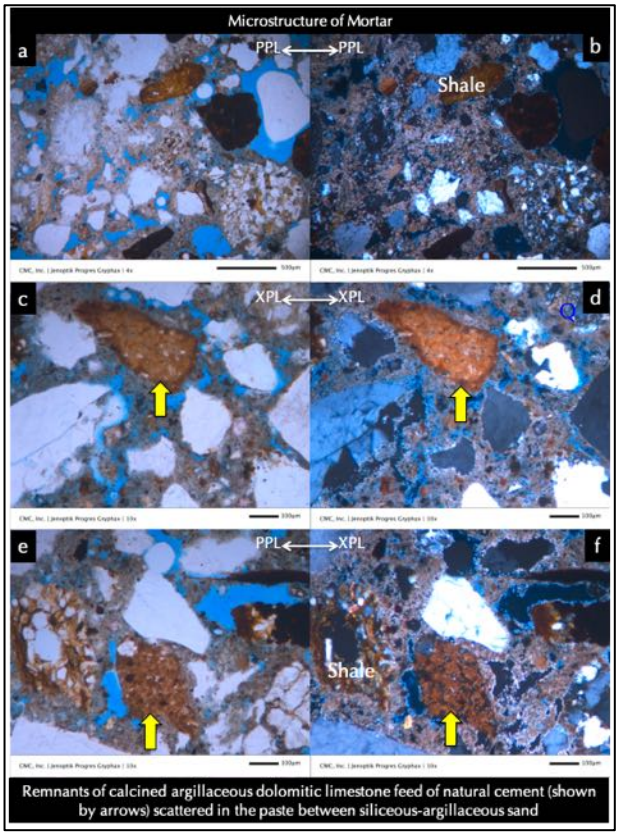


Figure 12: Microstructure of cement paste.

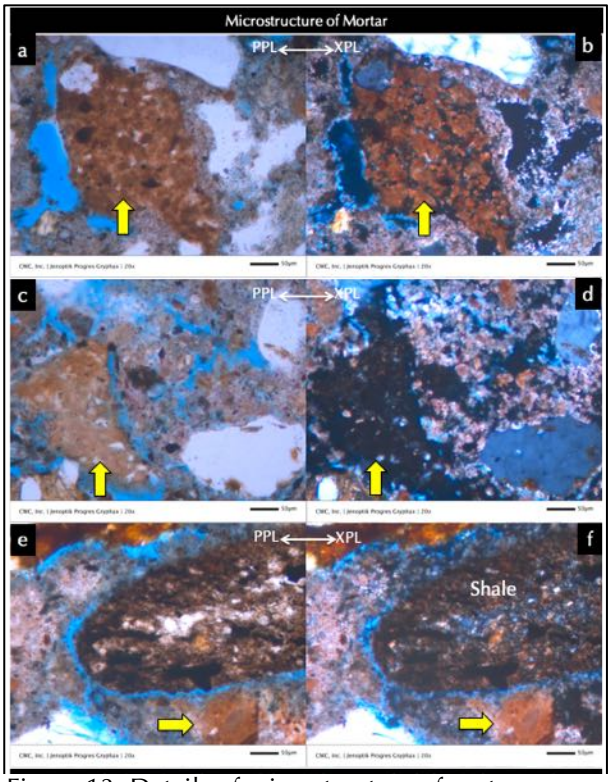


Figure 13: Details of microstructure of paste.

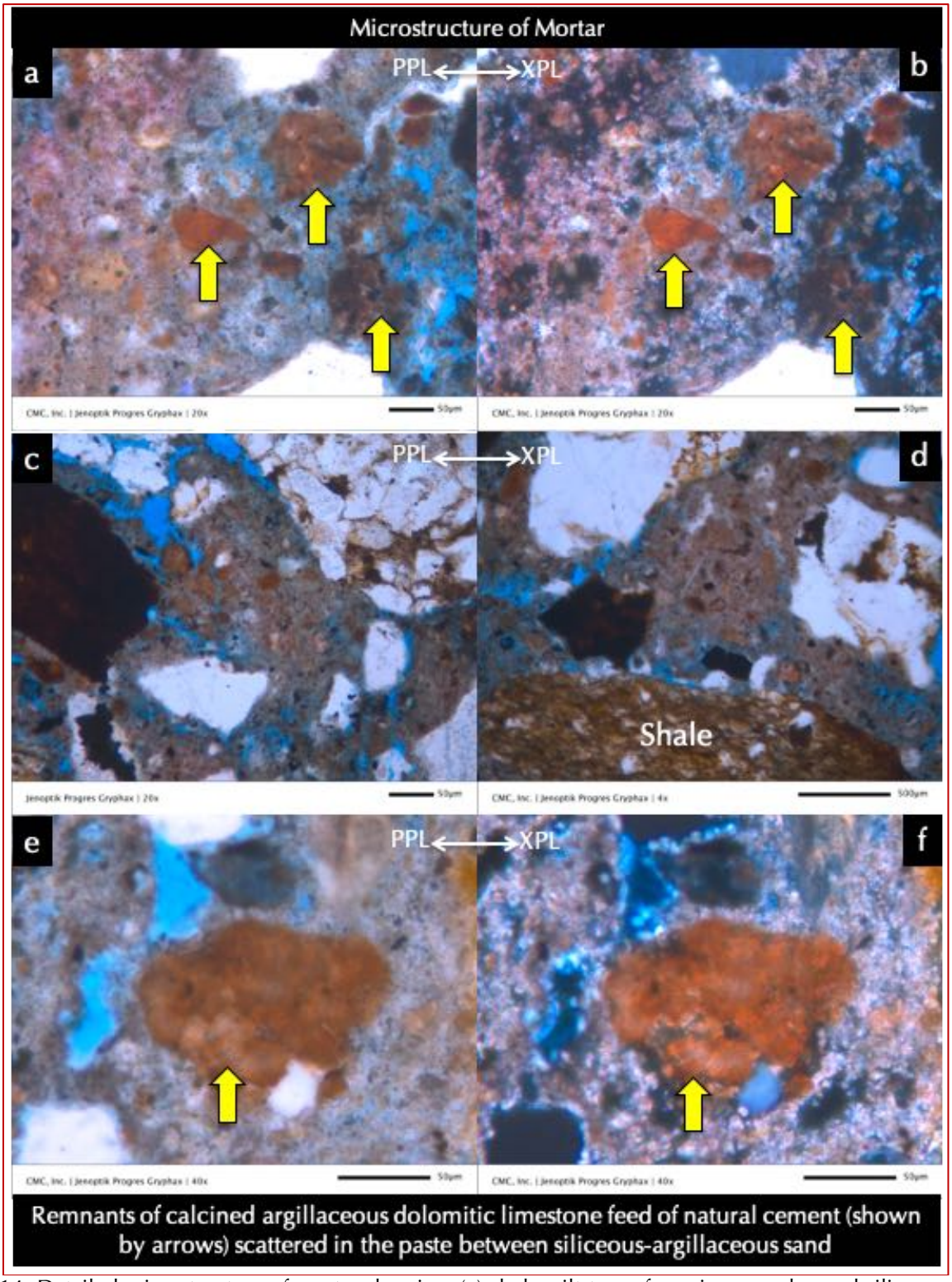


Figure 14: Detailed microstructure of mortar showing: (a) shale, siltstone, ferruginous rocks, and siliceous quartz particles in sand, (b) severely altered, carbonated, and leached interstitial paste that shows a porous microstructure from leaching, and, (c) residual calcined dolomitic limestone particles representing residual natural cement particles having relic rhombic crystals of dolomite with dark reddish-brown iron enrichment at the boundaries (many are marked with arrows). Paste microstructure is characteristic of a historic lime and natural cement mortar that has undergone leaching and carbonation during service.

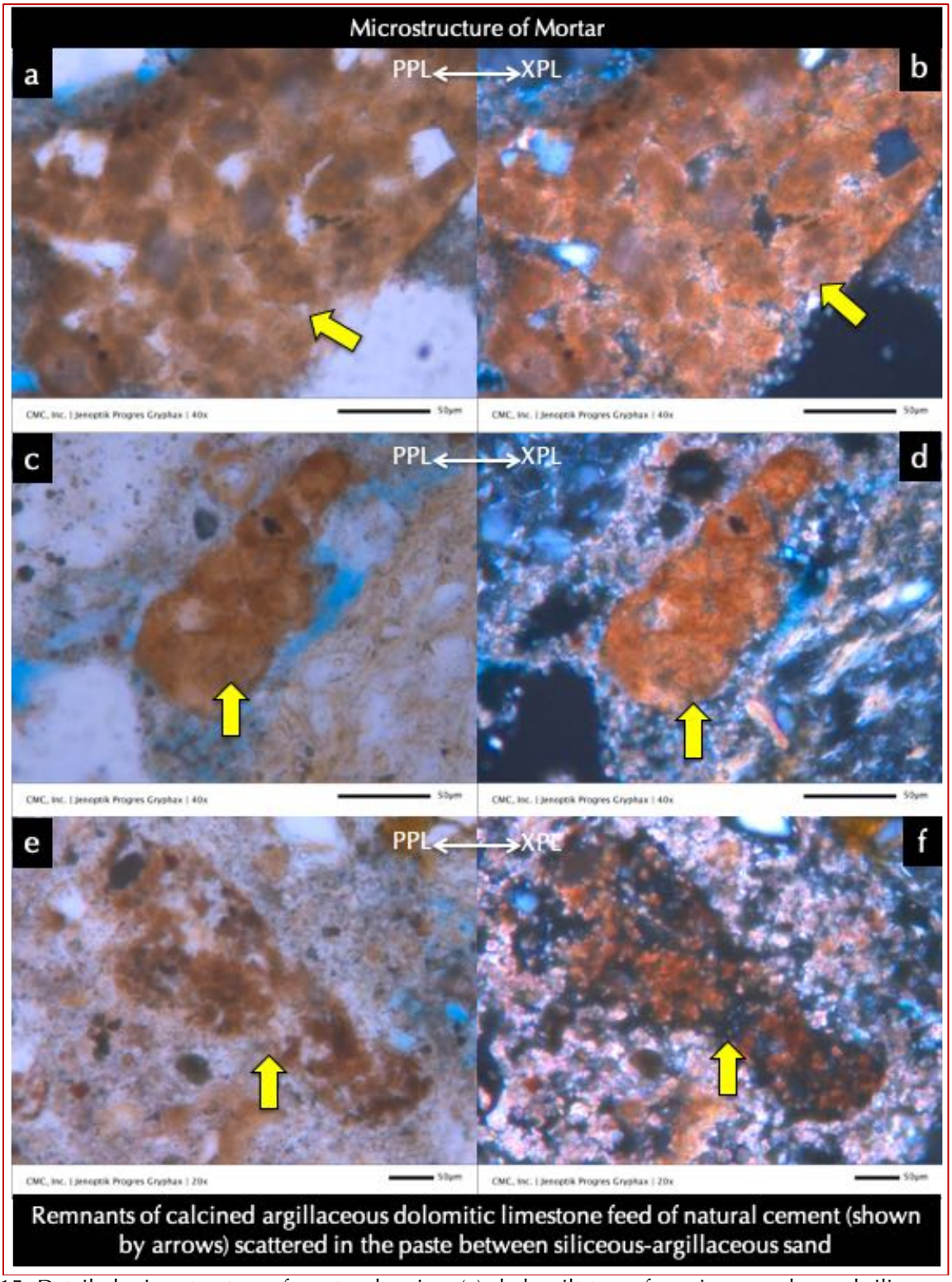


Figure 15: Detailed microstructure of mortar showing: (a) shale, siltstone, ferruginous rocks, and siliceous quartz particles in sand, (b) severely altered, carbonated, and leached interstitial paste that shows a porous microstructure from leaching, and, (c) residual calcined dolomitic limestone particles representing residual natural cement particles having relic rhombic crystals of dolomite with dark reddish-brown iron enrichment at the boundaries (many are marked with arrows). Paste microstructure is characteristic of a historic lime and natural cement mortar that has undergone leaching and carbonation during service.

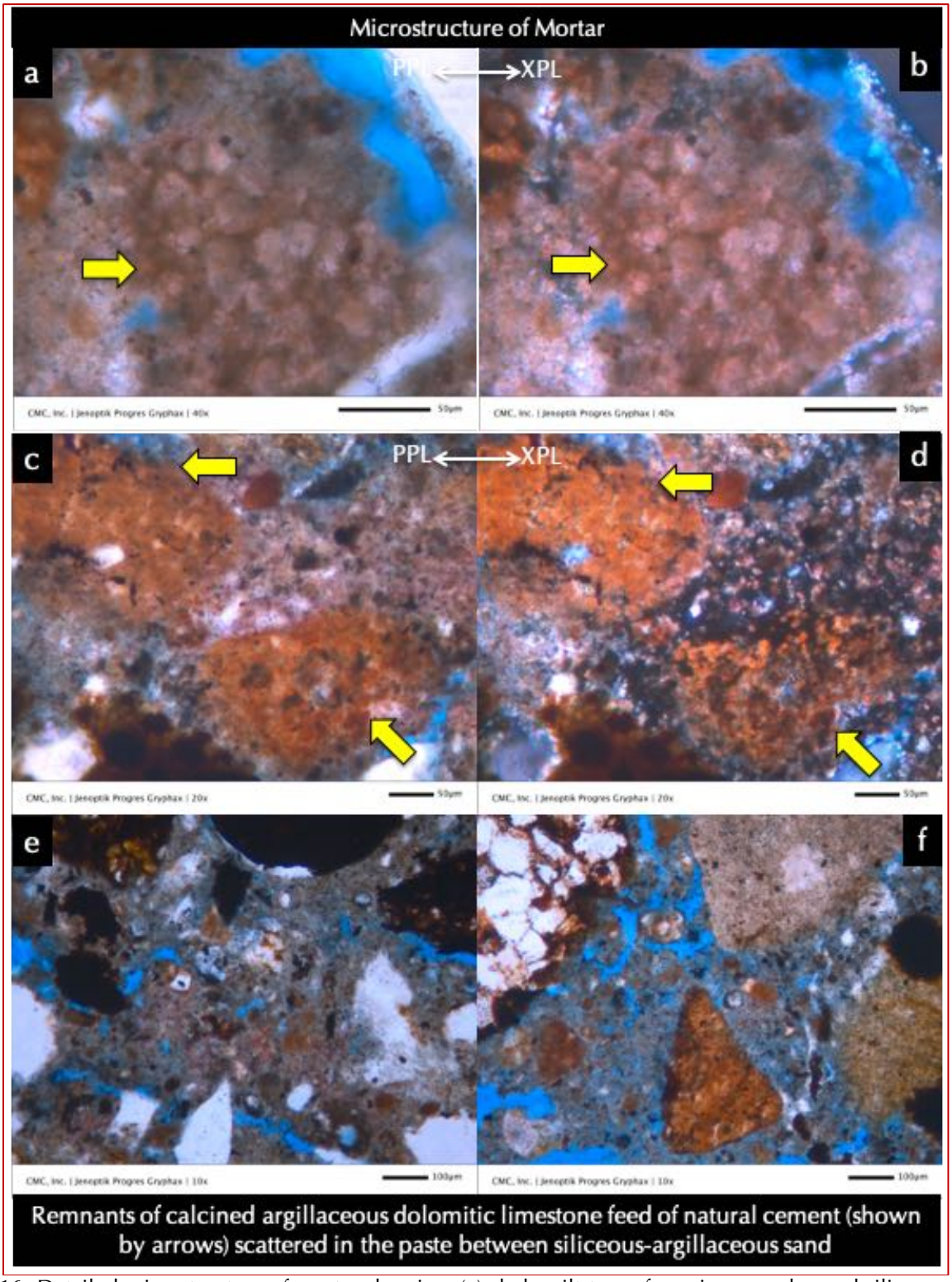


Figure 16: Detailed microstructure of mortar showing: (a) shale, siltstone, ferruginous rocks, and siliceous quartz particles in sand, (b) severely altered, carbonated, and leached interstitial paste that shows a porous microstructure from leaching, and, (c) residual calcined dolomitic limestone particles representing residual natural cement particles having relic rhombic crystals of dolomite with dark reddish-brown iron enrichment at the boundaries (many are marked with arrows). Paste microstrucutre is characteristic of a historic lime and natural cement mortar that has undergone leaching and carbonation during service.

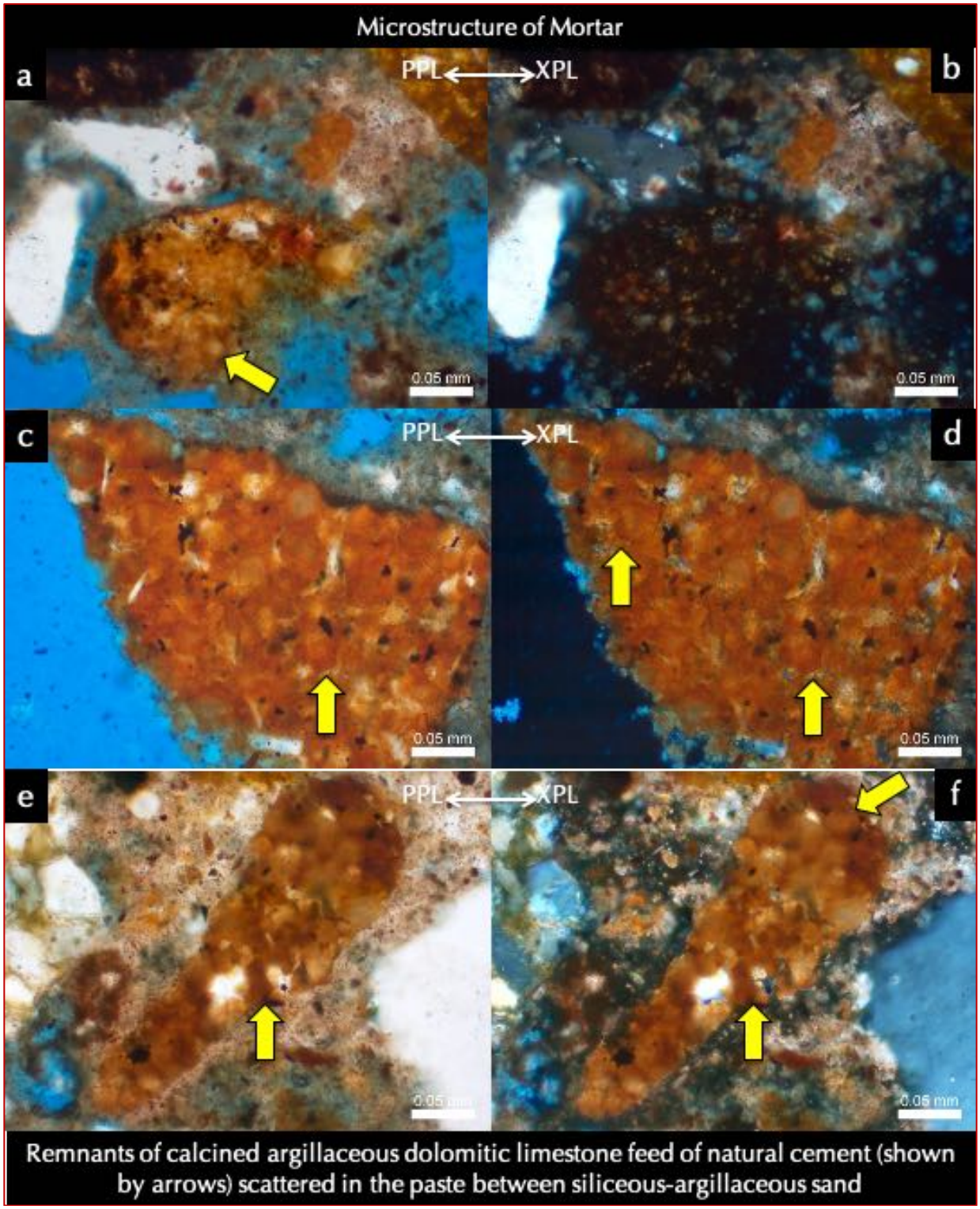


Figure 17: Detailed microstructure of mortar showing residual calcined dolomitic limestone particles representing residual natural cement particles having relic rhombic crystals of dolomite with dark reddish-brown iron enrichment at the boundaries (many are marked with arows). Also present are trydimite and cristobalite forms of fine silica inclusions in the calcined natural cement residues. Paste microstrucutre is characteristic of a historic lime and natural cement mortar that has undergone leaching and carbonation during service.

## Paste Compositions and Microstructure From SEM-EDS

Figure 18 shows backscatter electron image (BSE, top), X-ray elemental maps (middle), and compositional analyses of paste from various areas on the backscatter image (bottom) of thin section of mortar from a scanning electron microscope.

BSE image shows sand particles that appear in medium gray with sharp boundaries, and paste in variable shades of gray from porous areas in darker tones than the denser and carbonated areas.

In X-ray elemental maps, siliceous components of sand are highlighted in Si-map, calcareous (lime) paste is highlighted in Ca-map, feldspar grains in sand are highlighted in Al map. Enrichment of magnesia in paste in Mg-map (not shown) indicate use of a dolomitic lime and natural cement in the binder.

Figure 18 shows compositional analyses of paste at various areas (at the tips of callouts) carefully selected to avoid any interference from sand particles or residual cement particles. Results of paste compositions are provided in the Table beneath.

Average paste composition after filtering interference from sand or cement particles are provided in the Table. Compositions of paste are indicative of leaching of lime with corresponding increase of silica, alumina, etc. in the leached mass.

The cementation indices (CI) of paste are calculated after Eckel (1922) as CI = $[(2.8*SiO_2)+(1.1*Al_2O_3)+(0.7*Fe_2O_3)]/[(CaO)+(1.4*MgO)]$, which measures relative hydraulicity of paste e.g., non-hydraulic lime pastes have very low CI (< 1) compared to Portland cement pastes (CI is >1). Results show very high CIs, which are characteristic of lime leaching in an altered mortar common in many historic mortars. CI varied across the paste depending on degree of mixing of natural cement and lime components and subsequent hydration and carbonation of components followed by degree of alterations (carbonation, leaching, etc.) that have caused some variations in major oxide contents of paste.

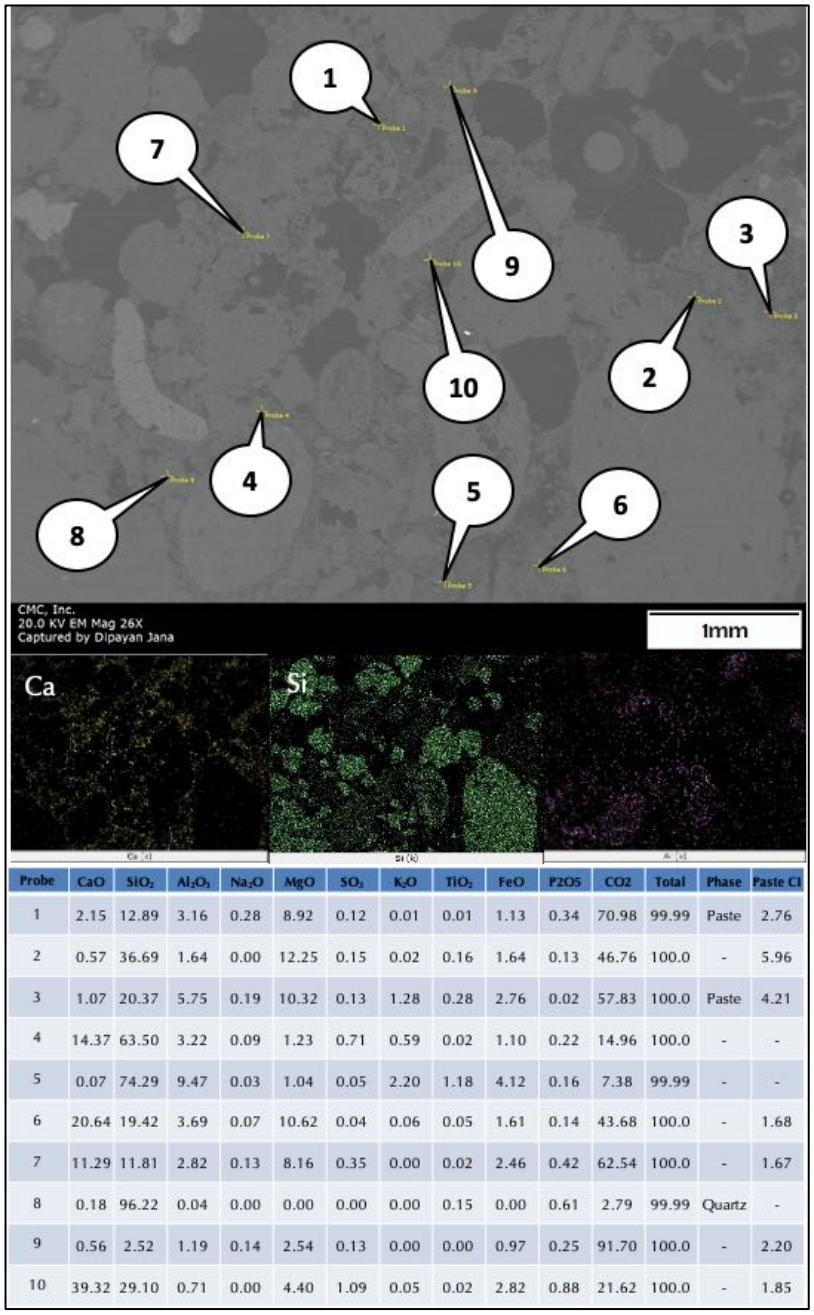


| Probe | CaO | $SiO_2$ | $Al_2O_3$ | $Na_2O$ | MgO | $SO_3$ | $K_2O$ | $TiO_2$ | FeO | P2O5 | CO2 | Total | Phase | Paste CI |
|---|---|---|---|---|---|---|---|---|---|---|---|---|---|---|
| 1 | 2.15 | 12.89 | 3.16 | 0.28 | 8.92 | 0.12 | 0.01 | 0.01 | 1.13 | 0.34 | 70.98 | 99.99 | Paste | 2.76 |
| 2 | 0.57 | 36.69 | 1.64 | 0.00 | 12.25 | 0.15 | 0.02 | 0.16 | 1.64 | 0.13 | 46.76 | 100.0 | - | 5.96 |
| 3 | 1.07 | 20.37 | 5.75 | 0.19 | 10.32 | 0.13 | 1.28 | 0.28 | 2.76 | 0.02 | 57.83 | 100.0 | Paste | 4.21 |
| 4 | 14.37 | 63.50 | 3.22 | 0.09 | 1.23 | 0.71 | 0.59 | 0.02 | 1.10 | 0.22 | 14.96 | 100.0 | - | - |
| 5 | 0.07 | 74.29 | 9.47 | 0.03 | 1.04 | 0.05 | 2.20 | 1.18 | 4.12 | 0.16 | 7.38 | 99.99 | - | - |
| 6 | 20.64 | 19.42 | 3.69 | 0.07 | 10.62 | 0.04 | 0.06 | 0.05 | 1.61 | 0.14 | 43.68 | 100.0 | - | 1.68 |
| 7 | 11.29 | 11.81 | 2.82 | 0.13 | 8.16 | 0.35 | 0.00 | 0.02 | 2.46 | 0.42 | 62.54 | 100.0 | - | 1.67 |
| 8 | 0.18 | 96.22 | 0.04 | 0.00 | 0.00 | 0.00 | 0.00 | 0.15 | 0.00 | 0.61 | 2.79 | 99.99 | Quartz | - |
| 9 | 0.56 | 2.52 | 1.19 | 0.14 | 2.54 | 0.13 | 0.00 | 0.00 | 0.97 | 0.25 | 91.70 | 100.0 | - | 2.20 |
| 10 | 39.32 | 29.10 | 0.71 | 0.00 | 4.40 | 1.09 | 0.05 | 0.02 | 2.82 | 0.88 | 21.62 | 100.0 | - | 1.85 |

Figure 18: Backscatter electron image (top), X-ray elemental maps of mortar for calcium, silicon, and aluminum (middle row) corresponding to the backscatter image at the top, and SEM-EDS compositional analyses of paste from around sand particles at the tips of callouts marked on the backscatter image.

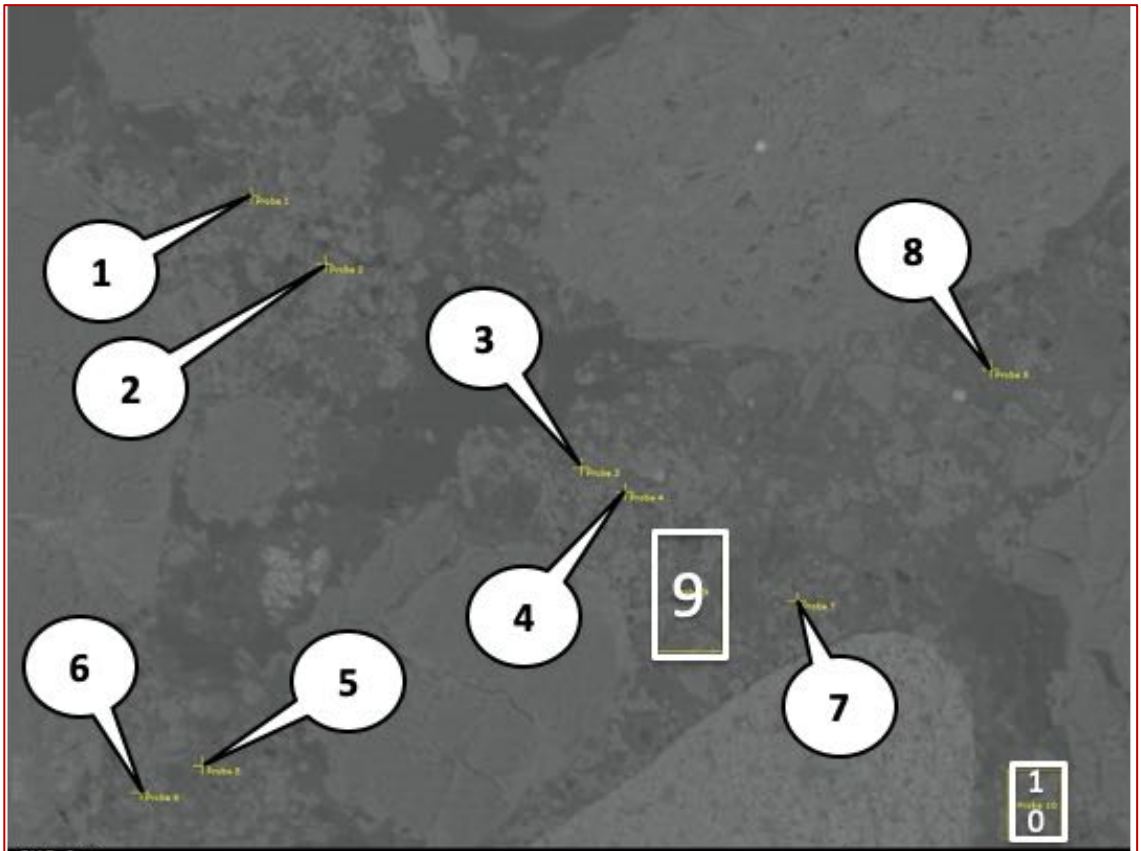


| Probe | CaO | $SiO_2$ | $Al_2O_3$ | $Na_2O$ | MgO | $SO_3$ | $K_2O$ | $TiO_2$ | FeO | P2O5 | CO2 | Total | Phase | Paste Cl |
|---|---|---|---|---|---|---|---|---|---|---|---|---|---|---|
| 1 | 7.52 | 20.42 | 6.25 | 0.01 | 11.57 | 0.14 | 0.30 | 0.06 | 3.46 | 0.06 | 50.21 | 100.0 | Paste | 2.80 |
| 2 | 35.90 | 12.49 | 4.03 | 0.10 | 8.16 | 0.11 | 0.47 | 0.15 | 2.49 | 0.41 | 35.69 | 100.0 | Paste | 0.87 |
| 3 | 82.04 | 3.06 | 0.24 | 0.00 | 4.58 | 0.66 | 0.00 | 0.00 | 2.46 | 0.49 | 6.46 | 100.0 | Paste | 0.12 |
| 4 | 0.47 | 37.26 | 23.10 | 0.02 | 4.19 | 0.33 | 1.97 | 0.20 | 19.65 | 0.44 | 12.37 | 100.0 | Paste | - |
| 5 | 0.00 | 94.16 | 0.28 | 0.00 | 0.00 | 0.23 | 0.00 | 0.00 | 0.00 | 0.38 | 4.94 | 100.0 | Quartz | - |
| 6 | 14.04 | 26.66 | 6.99 | 0.00 | 11.90 | 0.21 | 0.41 | 0.04 | 6.54 | 0.25 | 32.96 | 100.0 | Paste | 2.83 |
| 7 | 10.69 | 30.41 | 5.10 | 0.03 | 14.68 | 0.87 | 0.29 | 0.03 | 3.54 | 0.28 | 34.08 | 100.0 | Paste | 2.98 |
| 8 | 1.25 | 36.08 | 7.26 | 0.00 | 17.41 | 0.21 | 0.10 | 0.05 | 6.00 | 0.24 | 31.39 | 100.0 | Paste | 4.42 |
| 9 | 22.74 | 15.47 | 4.81 | 0.00 | 10.32 | 0.37 | 0.25 | 0.03 | 4.04 | 0.07 | 41.89 | 100.0 | Paste | 1.38 |
| 10 | 21.81 | 19.30 | 3.09 | 0.01 | 9.96 | 0.66 | 0.08 | 0.31 | 4.55 | 0.56 | 39.67 | 100.0 | Paste | 1.70 |

Figure 19: SEM-EDS compositional analyses of paste around sand particles from the tips of callouts marked on the backscatter electron image of the mortar. Paste compositions are characteristic of natural cement and lime that are characteristic of many historic mortars.

## Air

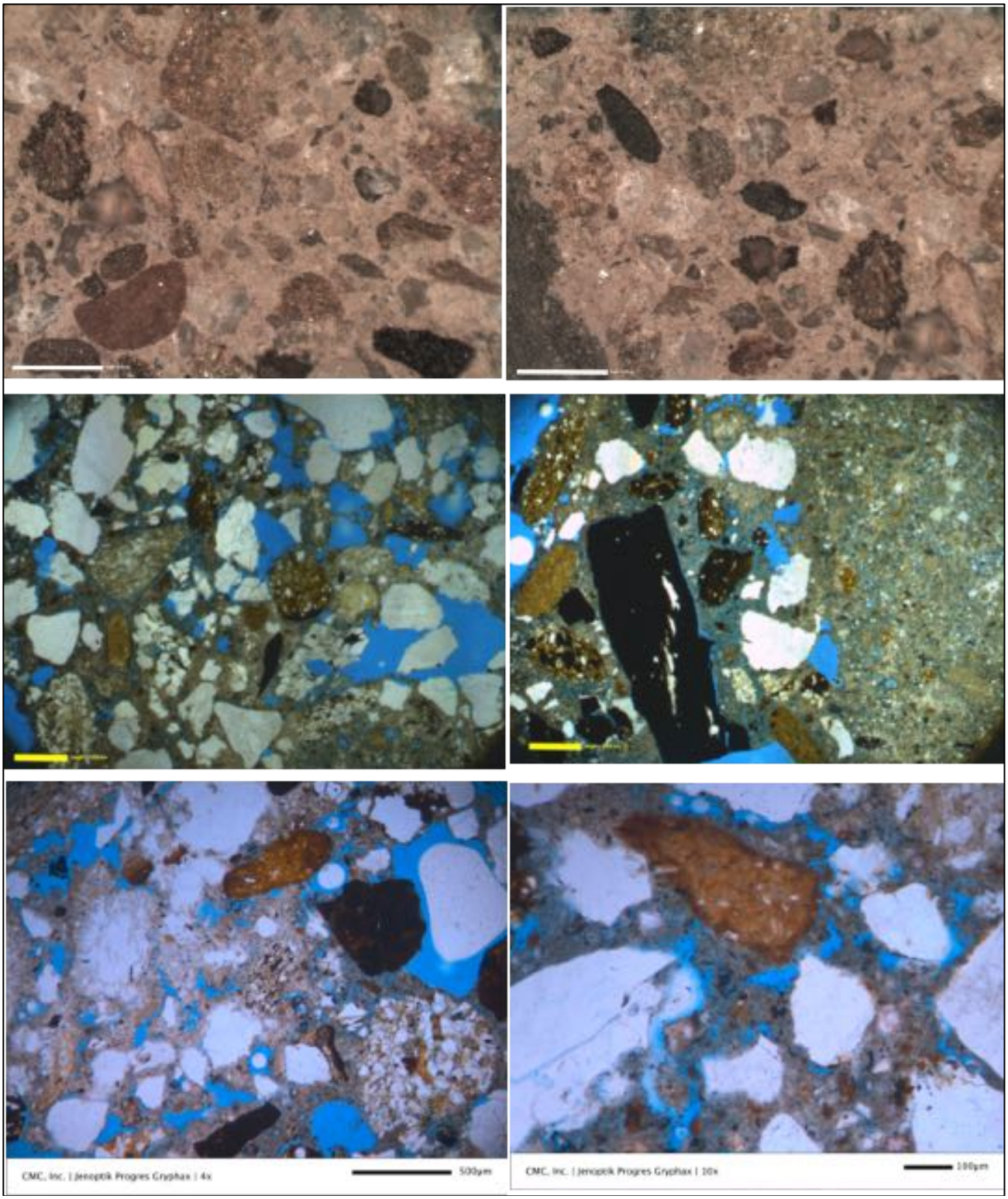


Figure 20: Photomicrographs of lapped section (top row), and blue dye-mixed epoxy-impregnated thin section of mortar (middle and bottom rows) showing lack of any spherical entrained air, whereas many coarse and irregularly-shaped entrapped air voids in mortar and overall non-air-entrained nature of mortar.

## Mineralogy of Mortar from XRD

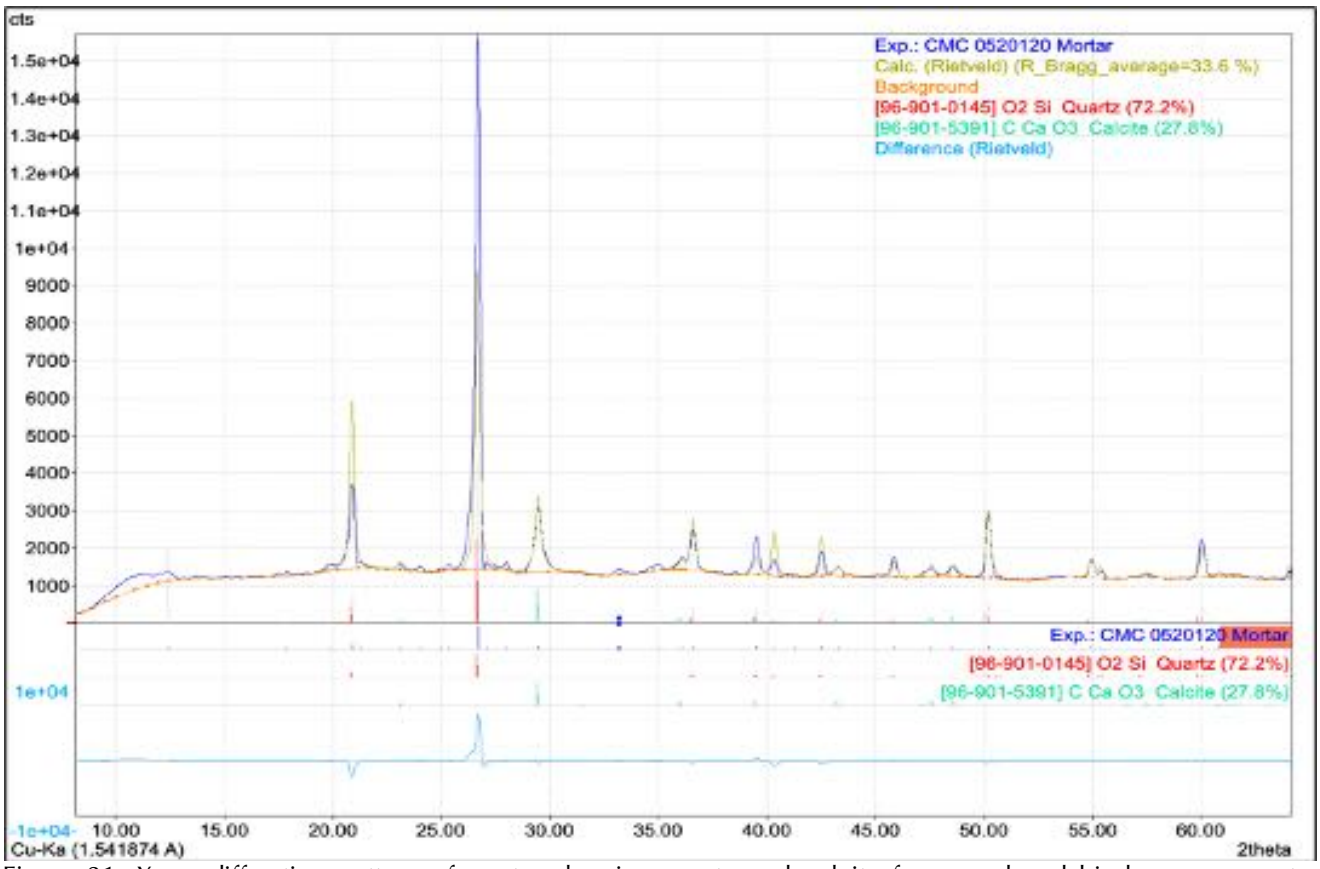


Figure 21: X-ray diffraction pattern of mortar showing quartz and calcite from sand and binder components, respectively.

Figure 21 shows X-ray diffraction pattern of the mortar, showing the dominance of quartz from siliceous component of sand, and calcite from carbonated paste. Many other phases, e.g., clay from argillaceous component of sand or silica polymorphs from calcined cement residues are not detected, which is probably due to use of the finest size fraction from the bulk sample that was used for XRD analysis where only the dominant constituents are populated.

## Composition of Mortar from XRF (Major Element Oxides), Acid & Alkali Digestion (Soluble Silica), Loss on Ignition (Free Water, Combined Water, Carbonation), and Acid-Insoluble Residue Content (Siliceous Sand Content)

Table 1 shows oxide compositions of mortar determined from pressed pellet of pulverized (< 45 micron size) bulk mortar in XRF. Dominance of silica (almost 50 percent) is a reflection of dominance of quartz sand in the mortar. Lime is contributed from carbonated paste and lime component in the binder. Sulfate is mainly from natural cement detected in optical microscopy, and alumina, and alkalis are contributed from both sand and paste. Magnesia is contributed mostly from the natural cement binder. Balance includes volatiles (combined $H_2O$, $CO_2$) not measured in XRF.

Natural cement and residues left after lime leaching of paste are responsible for the soluble silica detected in the XRF analysis of filtrate (2.357% $SiO_2$) after digestions in cold-HCl and hot-NaOH.

Acid-insoluble residue content of mortar is determined after digesting pulverized (<0.3 mm size) fragments of mortar in hydrochloric acid. Losses on ignition of a separate aliquot of pulverized mortar to 110°C, 550°C, and 950°C correspond to free water, combined (hydrate) water, and degree of carbonation, respectively.

Due to the presence of siliceous, argillaceous, and ferruginous components in the sand (as determined from petrography) and no calcareous components, the determined acid-insoluble residue content (67 percent) is considered corresponding to the sand content of the mortar. The loss on ignition at 550°C corresponds to the loss of hydrate water including water present in altered paste. The loss on ignition at 950°C corresponds to degree of carbonation of carbonated lime and cement paste.

| Mortar Composition | Values | Methods |
|---|---|---|
| Silica - $SiO_2$ | 51.9 | XRF |
| Alumina - $Al_2O_3$ | 6.89 | XRF |
| Iron - $Fe_2O_3$ | 7.42 | XRF |
| Lime - CaO | 10.0 | XRF |
| Magnesia - MgO | 5.18 | XRF |
| Sodium - $Na_2O$ | 0.236 | XRF |
| Potassium - $K_2O$ | 1.12 | XRF |
| Titanium - $TiO_2$ | 0.621 | XRF |
| Phosphorus - $P_2O_5$ | 0.138 | XRF |
| Sulfate - $SO_3$ | 0.044 | XRF |
| Balance | 16.4 | XRF |
| Total | 100 | XRF |
| Soluble Silica in filtrates of Cold-HCl and Hot-NaOH digested mortar | 2.357 | XRF |
| Acid-Insoluble Residue | 67.0 | Gravimetry |
| Loss on Ignition @ 110°C | 0.90 | Gravimetry |
| Loss on Ignition @ 550°C | 5.60 | Gravimetry |
| Loss on Ignition @ 950°C | 6.70 | Gravimetry |

Table 1: Bulk oxide compositions and soluble silica content of mortar from XRF, and acid-insoluble residue content and losses on ignition from gravimetry.

## Thermal Analyses

Figure 22 shows TGA (in bold black), DSC (in dotted red), and DTG (in dashed blue) curves of mortar showing losses in weight due to decompositions (loss of water and carbon dioxide) of various phases during controlled heating in a Mettler-Toledo's simultaneous TGA/DSC 1 unit from 30ºC to 1000ºC in a ceramic crucible (alumina 70µl, no lid) at a heating rate of 10ºC/min in a nitrogen purge at a rate of 75 mL/min.

Dehydration and decarbonation reactions are marked as endothermic peaks in the DTG curve, whereas alpha to beta-form polymorphic transition of quartz is marked at the characteristic temperature of 576ºC in the DSC curve.

In the DTG curve, successive losses in weights are detected at (i) 85ºC (Peak #1) from free water, and (ii) a series of small endothermic peaks from 180 to 497ºC (Peak #2 to 5) from dehydroxylation of clays, hydrates, and sulfate, Peak #7 at 780ºC is from carbonation of fine-grained calcite in carbonated matrix. DSC curve shows polymorphic transition from alpha to beta form of quartz at 576ºC from silica (quartz) sand (Peak #6).

Quantitative estimates of quartz and dolomite/calcite are determined to be 44.7 and 13.2 percent, respectively.

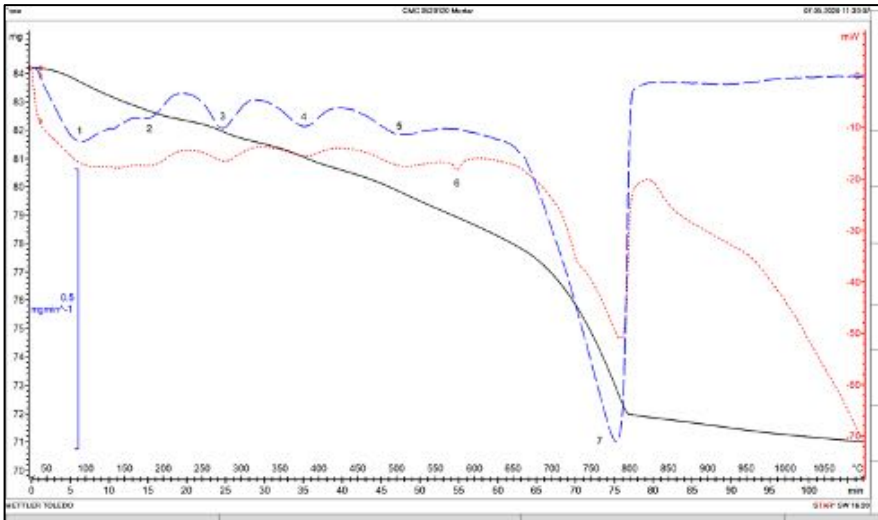

| Endothermic/ Polymorphic Peaks# | Peak Position (°C) | Phase |
|---|---|---|
| 1 (DTG) | 85.07 | Free Water |
| 2 (DTG) | 180.2 | Hydrate |
| 3 (DTG) | 273.09 | Hydrate |
| 4 (DSC) | 379.05 | Hydrate |
| 5 (DTG) | 497.5 | Hydrate |
| 6 (DSC) | 576.04 | Quartz, 44.7% |
| 7 (DTG) | 780.3 | Calcite, 13.2% |

| T(°C) | Up to 120°C | 120°C to 200°C | 200°C to 600°C | > 600°C |
|---|---|---|---|---|
| Phases | Hygroscopic Water | Water from Hydrated Salts | Structural Water From Hydraulic Components | $CO_2$ from decomposition of carbonates |
| Mass Loss (%) from TGA | 0.99 | 0.98 | 4.60 | 8.61 |

Figure 22: Thermal analyses of mortar.

## Ion Chromatography

Figure 23 shows anion chromatogram of water-soluble salts in mortar after digesting a gram of pulverized mortar in distilled water for 30 minutes at a temperature below boiling, followed by continued digestion in water at the ambient laboratory condition for 24 hours. The filtrate was analyzed by ion chromatography.

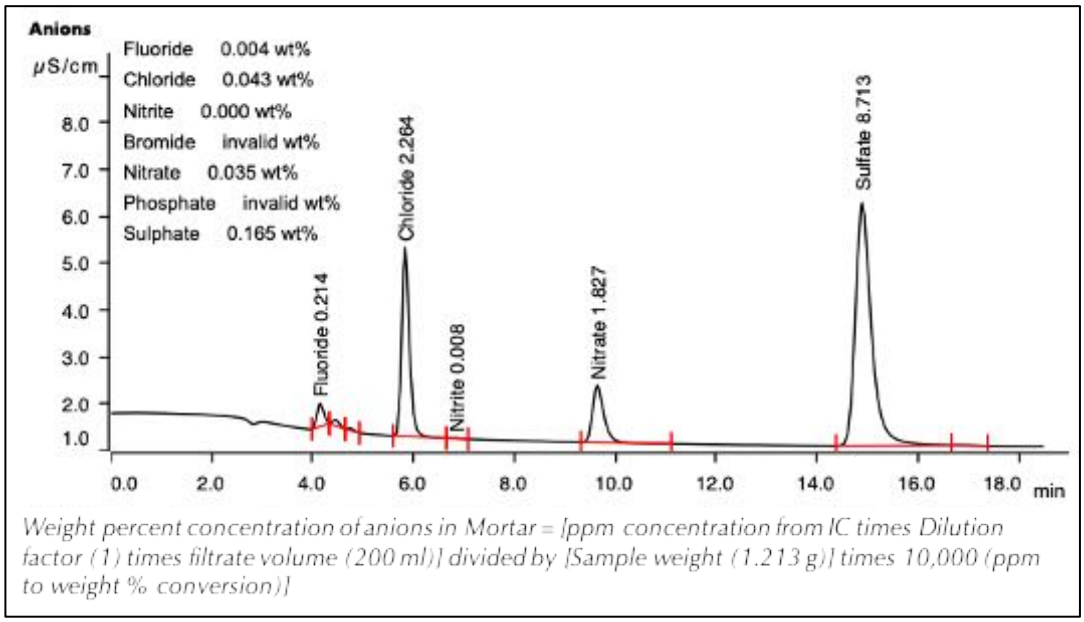


Figure 23: Water-soluble salts (anions) in mortar.

Results showed negligible chloride (0.043%), nitrate (0.0.035%), and reasonable sulphate (0.165%) contents due to use of natural cement.

# DISCUSSIONS

## Type of Mortar & Its Ingredients

Optical microscopy has determined the natural cement and dolomitic lime composition of the historic mortar consisting of lime putty, natural cement, and mixed siliceous-argillacoeus-ferruginous sand, where the siliceous component of sand is crushed silica whereas argillacoeus-ferruginous components are from natural river sand. Mortar compositions are determined from (a) characteristic mineralogies of sand and binder, (b) hydrated, carbonated, and severly leached microstructure and composition of paste containing a very porous fine-grained carbonated matrix with patches of leached paste and a few scattered residual natural cement particles, and (c) mixed crushed and natural sand of argillaceous-siliceous compositions. Dominance of argillacoeus (shale, argillaceous silstone) components in sand are potentially deleterious to volume instability of mortar during exposures to miosture. Too much clay-rich components in sand increases the water demand of mortar mix and risk of unsoundness during exposures to mosture, wetting and drying and freezing and thawing cycles during exposures in a moist outdoor environment. Angular quartz and rounded shale particles in sand indicates incorportaiton of crushed silica sand and natural river sand, respectively. Optical and SEM-EDS analyses of paste confirmed the presence of natural cement made using calcination of impure dolomitic limestone where many residual natural cement particles retained the original rhombic crystal shapes of dolomite grains in original dolomitic limesotne feed (with evidence of elemental migraiton during calcination process e.g., from reddish brown iron enrichment at the rims of dolomite grains to high-temperature silica polymorphs as fine insterstitial grains between calcined dolomite grains), and, doliomitic lime as the binder components. Paste has been variably leached during service. XRD analysis of the finest size fraction of mortar received showed the dominance of quartz from silica component, and calcite from carbonated paste but no potentially deletruous salts. XRF studies of acid and alkali-digested filtrates of mortar showed noticeable soluble silica from use of hydraulic (natural) cement component in the binder. High magnesia composition of paste, and overall high MgO content of mortar are consistent with use of a natural cement and dolomitic lime component in the binder. Results obtained from microscopy, chemical analyses, and finally thermal analyses are all consistent, confirmatory to each other, and provided a comprehensive understanding of mortar, which was determined to be prepared from mixing natural cement, dolomitic lime, and mixed crushed silica and argillaceous-ferruginous river sand particles for this historic mortar.

## Mix Calculations

Aided with the data obtained from petrography and chemical analyses of mortar, the following table first summarizes all chemical data, followed by calculations of proportions of various ingredients in the mortar from a set of assumed compositions and bulk densities of the ingredients:

| Mortar Compositions & Mix Proportion | Natural Cement - Lime – Mixed Sand Mortar |
|---|---|
| Chemical Compositions | |
| Soluble Silica, $SiO_2$ (%) | 2.357 |
| Bulk Calcium Oxide, CaO (%) | 10.0 |
| Bulk Magnesium Oxide, MgO (%) | 5.18 |
| Acid-Insoluble Residue (%) | 67.0 |
| Loss on Ignition: From 0°C to 110°C (Free Water) (%) | 0.90 |
| Loss on Ignition: From 110-550°C (Combined Water) (%) | 5.60 |
| Loss on Ignition: From 550-950°C (Carbonation, $CO_2$) (%) | 6.70 |
| Magnesium Hydroxide (Brucite) (%) | - |
| Assumed Compositions & Densities | |
| Natural Cement – From Soluble Silica ($SiO_2$) (%) See Table 7 | 26.6 percent soluble silica in natural cement |
| Bulk Density of Natural Cement, (lbs./ft.$^3$) | 75 |
| Bulk Density of Lime, (lbs./ft.$^3$) | 40 |

| Mortar Compositions & Mix Proportion | Natural Cement - Lime – Mixed Sand Mortar |
|---|---|
| Hydrated Lime or Lime putty, after assigning CaO to natural cement and assuming 35.6% CaO in natural cement (see Table 7) | From CaO content, after assigning CaO for Natural Cement and assuming 35.6% CaO in Natural Cement, and converting the residual CaO to lime $Ca(OH)_2$ by multiplying the residual CaO with the factor 1.322 (mol. wt. of lime to CaO = 74.03/56 = 1.322) |
| Bulk Density of Sand, (lbs./ft.$^3$) | 80 |
| Calculated Volumetric Proportions | |
| Natural Cement Content (%) | Natural Cement Content from Soluble Silica Data = 100(2.357/26.6) = 8.86%; |
| Hydrated Lime or Lime putty, assuming 35.6% CaO in natural cement, see Table 7 | 1.322 × [CaO content in mortar i.e. 10.0 – (8.86 i.e. cement content × 0.356)] = 9.05 |
| Sand Content (%) | 67 (Siliceous sand from acid-insoluble residue content) |
| Natural Cement Volume | 8.86/75 = 0.118 |
| Hydrated Lime Volume | 9.05/40 = 0.226 |
| Sand Volume | 67/80 = 0.837 |
| Relative Volumes of Cement to Lime to Sand | Natural Cement: Lime: Sand = 0.118: 0.226: 0.837 = 1: 1.9: 7.1 (2.4 times the sum of separate volumes of cement and lime) |

Table 2: Calculations of mix proportion of mortar, by volume, from the determined chemical compositions, and, assumed compositions and bulk densities of mortar ingredients.

Chemical composition of Rosendale natural cement used in the above calculations is derived from an average composition of Rosendale cement from Eckel 1922 (average of 23 analyses of Rosendale natural cement, from Page 247, Table 121 of Eckel 1922):

| Rosendale Natural Cement | $SiO_2$ | $Al_2O_3$ | $Fe_2O_3$ | CaO | MgO | Alkalis | Cl |
|---|---|---|---|---|---|---|---|
| Eckel (1922) | 26.66 | 8.02 | 3.98 | 35.60 | 18.30 | 4.05 | 1.42 |

Table 3: Average chemical composition of 23 analyses of Rosendale natural cement from Eckel 1922.

The soluble silica content of the mortar provided a natural cement content of 8.86 percent, by assuming 26.6% soluble silica in natural cement from an average chemical composition of Rosendale cement from Eckel (1922). Lime content is determined from the bulk calcium oxide content of mortar, after assigning CaO for natural cement and assuming 35.6% calcium oxide in natural cement (from Eckel 1922), and converting the residual CaO to lime i.e. $Ca(OH)_2$ by multiplying the residual CaO with the conversion factor 1.322 [ratio of mol. wt. of lime i.e. $Ca(OH)_2$ to CaO is 74.03/56 = 1.322]. Since the sand is determined to be mixed siliceous (quartz-quartzite)-argillaceous (shale, siltstone)-ferruginous sand, and contains no calcareous component, the sand content is determined from the hydrochloric acid-insoluble residue content of mortar. Assuming bulk densities of natural cement, lime, and sand as 75, 40, and 80 lbs./ft$^3$, respectively, the volumetric proportion of natural cement to lime to sand is calculated to be 1-part natural cement (similar to Rosendale cement, modern equivalent is Rosendale 10C cement from Edison Coatings, Inc.) to less than 2-part dolomitic lime to 7-part sand. Sand content is 2.4 times the sum of separate volumes of cement and lime. These calculated volumetric proportions are not representative of any modern-day ASTM C 270 mortars but very common in many historic natural cement and lime mortars.

## Condition

Leaching of lime is noted which is not uncommon for many historic mortars where paste constitutes an essentially altered product due to elemental migration and alteration of paste during service as opposed to normal hydration and carbonation products of binders used in modern masonry mortars. As opposed to paste, however, sand represents more original composition, which is mixed argillaceous, siliceous, and ferruginous in nature. Overall the mortar is found to be present in reasonably altered condition that has experienced chemical alterations during its service.

## Replacement Mix for Mortar

Based on the above determination of mix proportions, possible tuck pointing mortar could be a natural cement-lime-sand mortar made using Rosendale natural cement, hydrated lime, and natural sand, conforming to the respective ASTM specifications of C 10, C 207, and C 144. The final choice of cement-lime-sand proportions would depend on the match in appearance, compositions, and properties with the original mortar.

Finally, the following section provides some additional information to consider during selection of an appropriate tuck-pointing mortar for a renovation project (many of which may not be applicable for the present project):

a) It is more important for a tuck-pointing mortar to be as close in physical, chemical, and mechanical properties to the existing mortar as possible than to conform to the ASTM C 270 specification for cement-lime or masonry/mortar cement mortars for unit masonry, which are for modern mortars to use for modern structural applications, and not necessarily applicable to renovation of historic lime/natural cement mortars. As a general rule, tuck-pointing mortar should be of same strength or softer than the original mortar.

b) Aggregate to use in the tuck-pointing mortar should be similar in color, gradation, appearance, mineralogy, and composition to the sand used in the existing mortar. Sand should be clean, free of any debris, unsound, or clay particles. Masonry sands should conform to the grading requirements of ASTM C 144. Avoid using sand that contains appreciable amounts of potentially alkali-silica reactive particles (e.g., chert) or argillaceous components (e.g., shale, siltstone) as found in the present mortar.

c) Binder for tuck-pointing mortar should be as close to the binder of the existing mortar in composition and properties as possible. For historic lime mortars, possible choices of binders are many:

   (i) Non-hydraulic high-calcium lime, or magnesian lime, or dolomitic lime (ASTM C 51) either in dry hydrate (hydrated lime) form, or as slurry or putty form;
   (ii) Hydraulic lime;
   (iii) Natural hydraulic lime (i.e. NHL 2, NHL 3.5, and NHL 5 with increasing strengths; feebly, moderately and eminently hydraulic natural hydraulic limes with increasing hydraulicity and 28-day compressive strengths from >2 to <7 MPa, to >3.5 to <10 MPa, to >5 to <15 MPa, respectively, produced from calcination of impure limestones having up to 10% clay, 11-20% clay, and 21-30% clay, respectively);
   (iv) Natural cements (conforming to specifications of ASTM C 10); or,
   (v) A combination of these,
   (vi) With or without a pozzolan (fly ash, slag, etc. if added strength and durability are needed).
   (vii) Portland cement, if used must be added at lesser proportions than lime, having proportions tested to find the best match in properties to the existing mortar.
   (viii) For breathability of the masonry wall, least stress to the existing mortar, accommodation of building movements, and good bond to masonry units, the binder of choice should be durable and similar in properties and performance to the existing binder having a good service record.

d) During applications of modern masonry mortars: (i) a job-mixed cement-lime mortar is commonly preferred by the architects than a masonry cement mortar, due to the better quality control of the former mortar; (ii) a masonry cement mortar is characteristically air-entrained, which may interfere with the bond to the adjacent masonry units, whereas, a non-air-entrained cement-lime mortar provides a better bond to the adjacent masonry units than an air-entrained masonry cement mortar, (iii) air entrainment usually provides

better workability and freeze-thaw durability to a mortar, however, as mentioned, it reduces the bond to the adjacent masonry units (depending on air content); (iv) for Portland cement-lime mortars, a Type M or S mortar (i.e. having a higher cement content than lime and hence a higher strength) is preferred for load-bearing applications than a Type N mortar (having a higher lime content than cement, hence provides better workability and water retention than a Type S or M mortar); (v) Portland cement to use in a mortar should conform to the specification of ASTM C 150; hydrated lime should conform to ASTM C 207; masonry/mortar cement, if used, should conform to ASTM C 91/C 1329; blended hydraulic cement, if used, should conform to ASTM C 595; (vi) relative proportions of Portland cement and lime will control the overall strength, workability, and bond properties of the repointing mortar.

e) A mortar strong in compressive strength might be desirable for a hard stone (such as granite), whereas a softer, more permeable lime mortar would be preferable for a historic wall of soft brick. Masonry deterioration caused by salt deposition results when the mortar is less permeable than the masonry unit. A strong mortar is still more permeable than hard, dense stone. However, in a wall constructed of soft bricks where the masonry unit itself has a relatively high permeability or vapor transmission rate, a soft, high lime mortar is necessary to retain sufficient permeability; using a strong mortar with a soft brick will result in spalling of bricks.

f) Mineral oxides or carbon-based pigments, if used and positively detected in an examined mortar, should be carefully replicated in the tuck pointing process to reproduce the color, texture, and appearance similar to the existing mortar (including the effects of atmospheric weathering on pigments). Dosage of pigment in the tuck-pointing mortars should be estimated from trial mixes of various dosages. If the original mortar contains a polymer component as suspected from microscopy, characterization of polymer could be done by FTIR-spectroscopy.

g) To have an optimum bond of a mortar to the adjacent masonry unit, relative proportions of cementitious materials and lime contents in the mortar should be carefully controlled. Lime provides the necessary workability and water retention, which are important in a mortar when used with a masonry unit of high suction). Therefore, the initial rate of absorption (or suction property) of the adjacent masonry units should also be carefully determined to match with the appropriate lime content in the mortar.

h) The final tuck pointing mortar should match in color and appearance to the existing mortars, and the closest match should be determined by trial and error on small test areas of the masonry wall to be tuck-pointed.

## REFERENCES

ASTM C 10, “Standard Specification for Natural Cement,” In Annual Book of ASTM Standards, Section Four Construction, Vol. 04.01 Cement; Lime; Gypsum; ASTM Committee C01 on Cement, 2017.

ASTM C 91, “Standard Specification for Masonry Cement,” In Annual Book of ASTM Standards, Section Four Construction, Vol. 04.01 Cement; Lime; Gypsum; ASTM Committee C01 on Cement, 2017.

ASTM C 144, “Standard Specification for Aggregate for Masonry Mortar,” In Annual Book of ASTM Standards, Section Four Construction, Vol. 04.05 Chemical-Resistant Nonmetallic Materials; Vitrified Clay Pipe; Concrete Pipe; Fiber-Reinforced Cement Products; Mortars or mortars and Grouts; Masonry; Precast Concrete; ASTM Committee C12 on Mortars or mortars for Unit Masonry, 2017.

ASTM C 1324, “Standard Test Method for Examination and Analysis of Hardened Masonry Mortar,” In Annual Book of ASTM Standards, Section Four Construction, Vol. 04.05 Chemical-Resistant Nonmetallic Materials; Vitrified Clay Pipe; Concrete Pipe; Fiber-Reinforced Cement Products; Mortars or mortars and Grouts; Masonry; Precast Concrete; ASTM Committee C12 on Mortars or mortars for Unit Masonry, 2017.

ASTM C 270, “Standard Specification for Mortar for Unit Masonry,” In Annual Book of ASTM Standards, Section Four Construction, Vol. 04.05 Chemical-Resistant Nonmetallic Materials; Vitrified Clay Pipe; Concrete Pipe; Fiber-Reinforced Cement Products; Mortars or mortars and Grouts; Masonry; Precast Concrete; ASTM Committee C12 on Mortars or mortars and Grouts for Unit Masonry, 2017.

ASTM C 1713, "Standard Specification for Mortars or mortars for the Repair of Historic Masonry," In Annual Book of ASTM Standards, Section Four Construction, Vol. 04.05 Chemical-Resistant Nonmetallic Materials; Vitrified Clay Pipe; Concrete Pipe; Fiber-Reinforced Cement Products; Mortars or mortars and Grouts; Masonry; Precast Concrete; ASTM Committee C12 on Mortars or mortars and Grouts for Unit Masonry, 2017.

ASTM C 51, "Standard Terminology Relating to Lime and Limestone (as used by the Industry)'" In Annual Book of ASTM Standards, Section Four Construction, Vol. 04.01 Cement; Lime; Gypsum; ASTM Committee C07 on Lime, 2017.

ASTM C 856, "Standard Practice for Petrographic Examination of Hardened Concrete," In Annual Book of ASTM Standards, Section Four Construction, Vol. 04.02; ASTM Subcommittee C 9.65, 2017.

ASTM C 1723, "Standard Guide for Examination of Hardened Concrete Using Scanning Electron Microscopy," In Annual Book of ASTM Standards, Section Four Construction, Vol. 04.02; ASTM Subcommittee C 9.65, 2017.

ASTM C 1329, "Standard Specification for Mortar Cement," In Annual Book of ASTM Standards, Section Four Construction, Vol. 04.01; ASTM Subcommittee C01.11, 2016.

ASTM C 150, "Standard Specification for Portland Cement," In Annual Book of ASTM Standards, Section Four Construction, Vol. 04.01; ASTM Subcommittee C01.10, 2018.

ASTM C 1489, "Standard Specification for Lime Putty for Structural Purposes," In Annual Book of ASTM Standards, Section Four Construction, Vol. 04.01; ASTM Subcommittee C07.02, 2015.

ASTM C 207, "Standard Specification for Hydrated Lime for Masonry Purposes," In Annual Book of ASTM Standards, Section Four Construction, Vol. 04.01; ASTM Subcommittee C07.02, 2011.

Bartos, P. Groot, C., and Hughes, J.J. (eds.), "Historic Mortars or mortars: Characteristics and Tests", Proceedings PRO12, RILEM Publications, France, 2000.

Boynton, R., *Chemistry and Technology of Lime and Limestone, 2nd edition*, John Wiley & Sons, Inc. 1980.

Brosnan, Denis, A., Characterization of Rosendale Mortars or mortars For Fort Sumter National Monument and Degradation of Mortars or mortars by Sea Water and Frost Action, Final Report, April 19, 2012.

Callebaut, K., Elsen, J., Van Balen, K., and Viaene, W., "Nineteenth century hydraulic restoration mortars or mortars in the Saint Michael's Church (Leuven, Belgium) Natural hydraulic lime or cement?" Cement and Concrete Research, V 31, pp 397-403, 2001.

Callebaut, K., Elsen, J., Van Balen, K., and Viaene, W., Historical and scientific study of hydraulic mortars or mortars from the 19th century. In International RILEM workshop on historic mortars or mortars: Characterization and Tests; Paisley, Scotland, 12th to 14th May 1999, Edited by Barton, P., Groot, C., and Hughes, J.J., Cachan, France, RILEM Publications, 2000.

Charloa, A.E., "Mortar analysis: A comparison of European procedures." US/ICOMOS Scientific Journal: Historic Mortars or mortars & Acidic Deposition on Stone, 3 (1), pp. 2-5, 2001.

Charola, A.E., and Lazzarin, L., Deterioration of Brick Masonry Caused by Acid Rain, ACS Symposium Series, Vol. 318, pp. 250-258, 2009.

Chiari, G., Torraca, G., and Santarelli, M.L., "Recommendations for Systematic Instrumental Analysis of Ancient Mortars or mortars: The Italian Experience", *Standards for Preservation and Rehabilitation*, ASTM STP 1258, S.J. Kelley, ed., American Society for Testing and Materials, pp. 275-284, 1996.

Doebley, C.E., and Spitzer, D., "Guidelines and Standards for Testing Historic Mortars or mortars", *Standards for Preservation and Rehabilitation*, ASTM STP 1258, S.J. Kelley, ed., American Society for Testing and Materials, pp. 285-293, 1996.

Eckel, Edwin, C., *Cements, Limes, and Plasters*, John Wiley & Sons, Inc. 655pp, 1922.

Edison, M.P. (Editor), *Natural Cement*, ASTM STP 1494, American Society for Testing and Materials, 2008.

Elsen, J., "Microscopy of Historic Mortars or mortars – A Review", *Cement and Concrete Research 36*, 1416-1424, 2006.

Elsen, J., Mertens, G., and Van Balen, K., Raw materials used in ancient mortars or mortars from the Cathedral of Notre-Dame in Tournai (Belgium), Eur. J. Mineral., Vol. 23, pp. 871-882, 2011.

Elsen, J., Van Balen, K., and Mertens, G., Hydraulicity in Historic Lime Mortars or mortars: A Review, In, Valek, J, Hughes, J.J., and Groot, W.P. (Eds.), Historic Mortars or mortars Characterisation, Assessment and Repair, RILEM Book series, Volume 7, pp. 125-139, Springer, 2012.

Erlin, B., and Hime, W.G., "Evaluating Mortar Deterioration", *APT Bulletin*, Vol. 19, No. 4, pp. 8-10+54, 1987.

Goins E.S., "Standard Practice for Determining the Components of Historic Cementitious Materials," National Center for Preservation Technology and Training, Materials Research Series, NCPTT 2004.

Goins, E.S., "A standard method for the characterization of historic cementitious materials." US/ICOMOS Scientific Journal: Historic Mortars or mortars & Acidic Deposition on Stone, # (1), pp. 6-7, 2001.

Groot, C., Ashall, G., and Hughes, J., Characterization of Old Mortars or mortars with Respect to their Repair, State-of-the-art Report of RILEM Technical Committee 167-COM, 2004.

Hughes, D.C., Jaglin, D., Kozlowski, R., Mayr, N., Mucha, D., and Weber, J., "Calcination of Marls to Produce Roman Cement", pp. 84-95, In, Edison, M.P. (Editor), *Natural Cement*, ASTM STP 1494, American Society for Testing and Materials, 2007.

Hughes, J.J., Cuthbert, S., and, Bartos, P., "Alteration Textures in Historic Scottish Lime Mortars or mortars and the Implications for Practical Mortar Analysis", *Proceedings of the 7th Euroseminar on Microscopy Applied to Building Materials*, Delft, pp. 417-426, 1999.

Hughes, R.E., and Bargh, B.L., The weathering of brick: Causes, Assessment and Measurement, A Report of the Joint Agreement between the U.S. Geological Survey and the Illinois State Geological Survey, 1982.

Jana, D., "Application of Petrography In Restoration of Historic Masonry Structures", In: Hughes, J.J., Lesie, A.B. and Walsh, J.A., eds. *Proceedings of 10th Euroseminar on Microscopy Applied to Building Materials*, Paisley, 2005.

Jana, D., "Sample Preparation Techniques in Petrographic Examinations of Construction Materials: A State-of-the-art Review", *Proceedings of the 28th Conference on Cement Microscopy*, International Cement Microcopy Association, Denver, Colorado, pp. 23-70, 2006.

Jedrzejewska, H., Old mortars or mortars in Poland: a new method of investigation, Studies in Conservation 5, pp. 132-138, 1960.

Leslie, A.B., and Hughes, J.J., "Binder Microstructure in Lime Mortars or mortars: Implications for the Interpretation of Analysis Results", *Quarterly Journal of Engineering Geology & Hydrogeology*, V. 35, No. 3, pp. 257-263, 2001.

Lubell, B., van Hees, Rob. P.J., and Groot, Casper J.W.P., The role of sea salts in the occurrence of different damage mechanisms and decay on brick masonry, Construction and Building Materials, Vol. 18, pp. 119-124, 2004.

Martinet, G., Quenee, B., Proposal for a useful methodology for the study of ancient mortars or mortars, Proceedings of the International RILEM workshop "Historic Mortars or mortars: Characteristics and tests," Paisley, pp. 81-91, 2000.

Mack, Robert, and Speweik, John P., *Preservation Briefs 2*, U.S. Department of the Interior, National Park Service Cultural Resources, Heritage Preservation Services, pp. 1-16, 1998.

Middendorf, B., Baronio, G., Callebaut, K, and Hughes, J.J., "Chemical-mineralogical and physical-mechanical investigation of old mortars or mortars, Proceedings of the International RILEM workshop "Historic Mortars or mortars: Characteristics and tests," Paisley, pp. 53-61, 2000.

Middendorf, B., Hughes, J.J., Callebaut, K., Baronio, G., and Papayanni, I., Mineralogical characterization of historic mortars or mortars, In. Groot, C., et al. (eds), Characterisation of Old Mortars or mortars with Respect to their Repair, State-of-the-art Report of RILEM Technical Committee 167-COM, pp. 21-36, 2004a.

Middendorf, B., Hughes, J.J., Callebaut, K., Baronio, G., and Papayanni, I., Chemical characterization of historic mortars or mortars, In. Groot, C., et al. (eds), Characterisation of Old Mortars or mortars with Respect to their Repair, State-of-the-art Report of RILEM Technical Committee 167-COM, pp. 37-53, 2004b.

Middendorf, B., Hughes, J.J., Callebaut, K., Baronio, G., and Papayanni, I., "Investigative Methods for the Characterization of Historic Mortars or mortars – Part 1: Mineralogical Characterization," *Materials and Structures*, Vol. 38, 2005a.

Middendorf, B., Hughes, J.J., Callebaut, K., Baronio, G., and Papayanni, I., "Investigative Methods for the Characterization of Historic Mortars or mortars – Part 2: Chemical Characterization," *Materials and Structures*, Vol. 38, pp 771-780, 2005b.

Sarkar, S.L., Aimin, Xu, and Jana, Dipayan, Scanning electron microscopy and X-ray microanalysis of Concretes, pp. 231-274, In, Ramachandran, V.S. and Beaudoin, J.J. Handbook of Analytical Techniques in Concrete Science and Technology, Noyes Publications, Park Ridge, New Jersey, 2000.

Speweik, J.P., *The History of Masonry Mortar in America 1720-1995*, 2010.

Stewart, J., and Moore, J., Chemical techniques of historic mortar analysis, Proceedings of the ICCROM Symposium "Mortars or mortars, Cements, and Grouts used in the Conservation of Historic Buildings," Rome, ICCROM, Rome, pp. 297-310, 1981.

Valek, J., Hughes, J.J., and Groot, C. (eds.), *Historic Mortars or mortars: Characterization, Assessment and Repair*, Springer, RILEM Book series Vol. 7, p. 464, 2012.

Valek, J., Hughes, J.J., and Groot, C. (eds.), Historic Mortars or mortars: Characterization, Assessment and Repair, Springer, RILEM Book series Vol. 7, 2012.

Van Balen, K., Toumbakari, E.E., Blanco, M.T., Aguilera, J., Puertas, F., Sabbioni, C., Zappia, G., Riontino, C., and Gobbi, G., "Procedures for mortar type identification: A proposal." In International RILEM workshop on historic mortars or mortars: Characteristics and Tests; Paisley, Scotland, 13th to 14th May 1999, edited by Barton, P., Groot, C., and Hughes, J.J., Cachan, France: RILEM Publications, 2000.

Vyskocilova, R., W. Schwarz, D. Mucha, D. Hughes, R. Kozlowski, and J. Weber, "Hydration processes in pastes of roman and American natural cements," *ASTM STP*, vol. 4, no. 2, 2007.

Weber, J., Gadermayr, N., Kozlowski, R., Mucha, D., Hughes, D., Jaglin, D., and Schwarz, W., Microstructure and mineral composition of Roman cements produced at defined calcination conditions, Materials Characterization, Vol. 58, pp. 1217-1228, 2007.

✪ ✪ ✪ END OF TEXT ✪ ✪ ✪

# END OF REPORT[2]

[2] The CMC logo is made using a lapped polished section of a 1930's concrete from an underground tunnel in the U.S. Capitol.